LAWRENCE
LIVERMORE
NATIONAL
LABORATORY

UCRL-TH-236712

Single-Mode VISAR

K. Krauter

November 21, 2007

Disclaimer

This work performed under the auspices of the U.S. Department of Energy by Lawrence Livermore National Laboratory under Contract DE-AC52-07NA27344.

Single-Mode VISAR

A Thesis
Presented to the Faculty of
California Polytechnic State University
San Luis Obispo

In Partial Fulfillment
Of the Requirements for the Degree
Master of Science in Electrical Engineering

By
Kerry Krauter
November 2007
Lawrence Livermore National Laboratory

UCRL-TH-236712

Approval Page

Title: Single-Mode VISAR

Author: Kerry Krauter

Date Submitted: November 28, 2007

Dr. Samuel Agbo _____
Advisor Signature

Dr. Dennis Derickson _____
Committee Member Signature

Dr. Xiaomin Jin _____
Committee Member Signature

Abstract

Single-Mode VISAR

by

Kerry Krauter

High energy-density physics (HEDP) experiments examine the properties of materials under extreme conditions. These experiments rely on the measurement of one or two velocities. These velocities are used to obtain Hugoniot relationships and thermodynamic equations of state. This methodology is referred to as "velocimetry" and an instrument used to measure the shock wave is called a "velocimeter" or a "(velocity) diagnostic."

The two most-widely used existing velocity diagnostics are; photonic Doppler velocimetry (PDV) and velocity interferometer system for any reflector (VISAR). PDV's advantages are a fast rise-time and ease of implementation but PDV has an upper velocity limit. Traditional implementations of VISAR have a rise time 10 times slower than PDV and are not easily implemented but are capable of measuring any velocity produced during HEDP experiments. This thesis describes a novel method of combining the positive attributes of PDV and VISAR into a more cost effective diagnostic called a Single-Mode VISAR (SMV). The new diagnostic will consist of PDV parts in a VISAR configuration. This configuration will enable the measurement of any velocity produced during shock physics experiments while the components used to build the diagnostic will give the diagnostic a fast rise time and make it easy to use. This thesis describes the process of building and testing the first single-mode VISAR. The tests include verifying the performance of the components and the diagnostic as a whole.

Acknowledgements

For generosity with his knowledge and time, I am deeply thankful to Pat Ambrose. His guidance on the development and building of the SMV was truly invaluable and I am grateful to count him among my mentors. I am also thankful to Gerard Jacobson for his help pulling parts out of thin air, for taking pictures, and for sharing his fiber handling expertise. Big thank-yous go to all the people in building 341 who have encouraged my research and helped provide several parts. Thanks to the people at site 300 for graciously lending me a capacitive discharge unit that worked. Thanks are due to Bruce Henderer of LLNL as well, for heading up the Cal Poly co-op program. I am deeply appreciative to the National Security Engineering Division at LLNL for sponsoring me during my thesis research. Thanks, of course, are due to Dr. Agbo for his time and effort as my advisor. Finally, I am deeply thankful to my family for their continuous support throughout my education. I am particularly grateful to my parents for exposing me to science and engineering as a kid, and encouraging me in the pursuit of my goals.

Table of Contents

List of Tables

List of Figures

CHAPTER 1 INTRODUCTION

For decades, national laboratories, universities, and numerous other research institutions have studied the properties of materials under extreme conditions. These high energy-density physics (HEDP) experiments involve inducing a shock wave in a material and then measuring the velocity of that shock wave as it propagates through a sample of the material or the velocity of the material itself after impact. High explosive driven plates, two stage gas guns, and z-pinch machines are a few methods of producing the desired shock wave in a target material. The data resulting from these types of experiments are used to obtain Hugoniot relationships and thermodynamic equations of state.

A Hugoniot describes the behavior of a shock wave in a material as a function of pressure and density. A material's equation of state describes the state of a material under prescribed conditions. Hugoniots and equations of state are highly regarded predictors of a material's behavior under specified conditions and therefore are widely used [1]. There are two distinct velocities that can be measured and used to provide the desired information; the actual shock velocity through the material and the mass velocity of the material. The shock wave and mass velocities in the sample material can vary greatly depending on the pressure induced by the driver. These velocities can vary from a few hundred m/s (~220mph) to tens of km/s (~20,000mph). The experiments involving the measurements of these velocities are generally over in a few microseconds. These shock physics experiments are sometimes called velocimetry experiments or simply shots. Since the velocity of the shock wave is required for the Hugoniot and the equation of state, significant research into methods of accurately measuring the velocity of the

shock wave is conducted. The methodology is referred to as "velocimetry" and an instrument used to measure the shock wave is called a "velocimeter" or a "(velocity) diagnostic." This thesis describes a novel velocimetry diagnostic developed in response to new requirements on the diagnostics used during HEDP experiments.

1.1 Velocimetry

Velocimeters can be purely electronic or optical in nature. Shorting pins are an example of a purely electronic velocimeter. While the shorting pins measure the arrival time of the shock wave rather than the actual velocity of the shock wave they can still be used to calculate the velocity of the shock wave through the target material. Shorting pins are open circuits that are butted up to the surface of a target material. The circuit remains open until the shock wave propagates through the material and crushes the end of the pin which shorts the circuit. The voltage across the pin is measured and recorded, thus providing a record of when the pin was shorted by the arriving shock wave [2]. Velocity data are obtained by placing the pins on multiple levels of the target material with a known thickness.

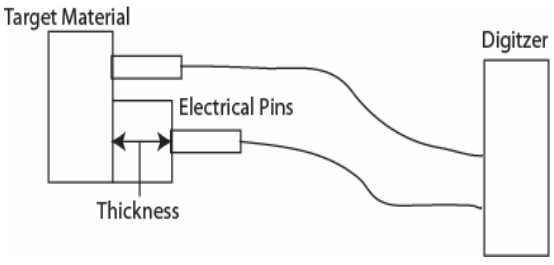

Figure 1-1 Electrical pins configured to measure shock velocity

The arrival time at each level is measured by a shorting pin and since the distance between levels is known the shock velocity information is easily calculated. This diagnostic has several limitations, which include an inability to track the shock velocity as it moves through the material and an inability to measure mass velocities. Optical velocimeters are often a better option than purely electrical velocimeters.

There are numerous types of optical velocimeters however, each distinct velocimeter operates on the same principle; that light is Doppler shifted upon encountering a moving surface and this light shift is proportional to the velocity of the moving surface.

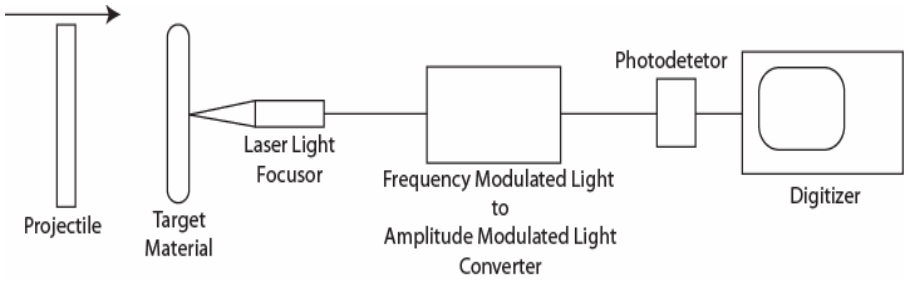

Figure 1-2 Components required in optical velocimeters

Optical velocimeters always contain at least a light source, a moving reflective surface, some method of converting the light from a frequency modulated signal into an amplitude modulated signal, a photodetector, and a digitizer [3-8]. The signal must be converted to amplitude modulated light since the frequency of the light signal is in the terahertz range, well above the capabilities of photodetectors currently available. The frequency modulated signal is typically mixed with either light from a local oscillator or split and mixed back with itself to convert the signal to amplitude modulated light.

Commonly used optical diagnostics include photonic Doppler velocimetery (PDV), and velocity interferometer system for any reflector (VISAR). In addition to the components listed, PDV and VISAR also require fiber probes or focusers. These probes are used to focus the laser light onto the target material and to collect and couple the shifted light into the fiber.

Optical diagnostics may be heterodyned or homodyned. Heterodyned diagnostics mix the Doppler shifted light with un-shifted light to produce amplitude modulated or beat signals. Homodyned diagnostics collect shifted light and split it between two distinct paths and then mix the light to produce amplitude modulated light at the photodetector. PDV is an example of a heterodyned diagnostic and VISAR is an example of a homodyned diagnostic.

1.1.1 Photonic Doppler Velocimetry (PDV)

PDV is a heterodyned diagnostic meaning that the Doppler shifted light is summed with a similar amount of un-shifted laser light. Often this un-shifted light is supplied by the back reflection of the probe. These two signals produce a beat frequency at the photodetector. According to Strand, the signal power at the photodetector can be described as;

$$I(t) = I_0 + I_d + 2\sqrt{I_0 I_d}\,\sin[f_b(t)\cdot 2\pi\cdot t + \varphi]$$

Where I_0 is un-shifted laser light intensity, I_d is the Doppler shifted light intensity, φ is the relative phase between the un-shifted and shifted light signals, and f_b is the beat frequency [4-5]. The un-shifted and shifted signals have frequencies in the terahertz range and consequently appear as continuous wave signals on the photodetector. The

beat frequency is the absolute value of the difference between the shifted and un-shifted light and this difference is typically in the GHz range and can be sensed by the photodetectors. The velocity of the surface is proportional to the beat frequency and is given by;

$$v(t) = \frac{cf_b(t)}{2f_0}$$

C is the speed of light and f_0 is the frequency of the un-shifted light. In the case of PDV, since we use 1550nm wavelength lasers, f_0 is 193.548 THz [4-5]. In PDV the electrical components limit the maximum velocity that can be measured since the bandwidth of the system must be capable of resolving the beat frequency. For example, to measure a 5 km/s velocity the system must be capable of resolving a 6.45 GHz frequency. A drawback to PDV is the need for very high speed electronics in order to measure high velocities. However, the use of commercially available single mode fiber optic components in PDV makes this diagnostic cost effective and easy to implement. Moreover, PDV has a very good rise-time, typically on the order of 100ps depending on the choice of detector, electronic cabling, and digitizer of course.

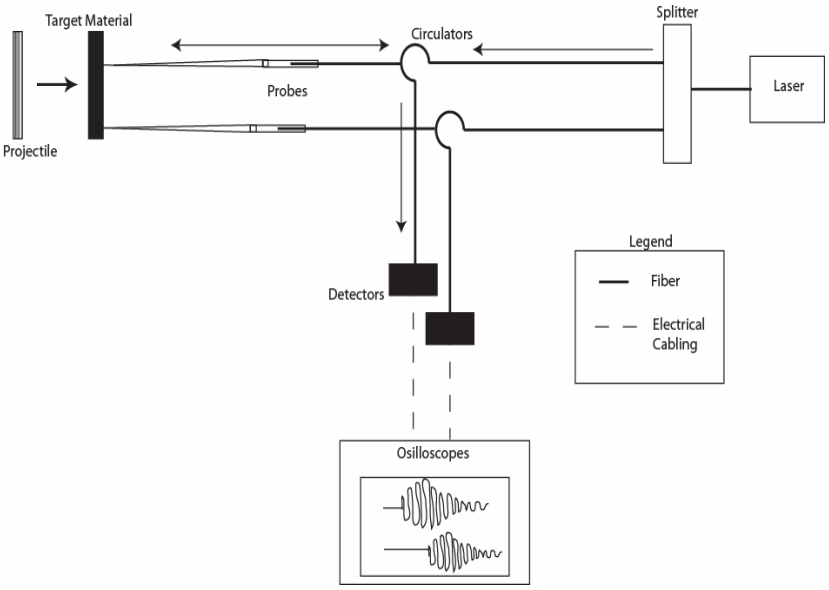

Figure 1-3 Principle configuration of the photonic Doppler velocimeter

1.1.2 Velocity Interferometer System for Any Reflector (VISAR)

In contrast to PDV, the VISAR is a homodyned diagnostic; meaning that the Doppler shifted light is divided between two optical paths of differing length and recombined at the photodetector. The VISAR diagnostic splits the Doppler shifted signal between two different path lengths and then recombines the signals at a beam splitter.

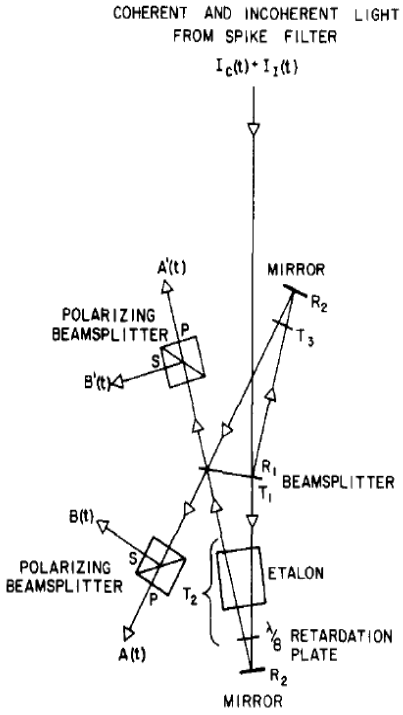

Figure 1-4 Principle configuration of a polarization split VISAR [6]

The two mixed signals are then, in some cases, polarization split to yield four data signals. The interference equation governs VISAR.

$$I = I_a + I_b + 2\sqrt{I_a I_b}\cos(\phi_{ab})$$

The four recorded data signals take the form of;

$$S_{1a} = P_{1a} + P_{1b} + 2\sqrt{P_{1a}P_{1b}}\cos(\phi\ )$$
$$S_{1b} = P_{1a} + P_{1b} - 2\sqrt{P_{1a}P_{1b}}\cos(\phi\ )$$
$$S_{2a} = P_{2a} + P_{2b} + 2\sqrt{P_{2a}P_{2b}}\cos(\phi\ +\beta)$$
$$S_{2b} = P_{2a} + P_{2b} - 2\sqrt{P_{2a}P_{2b}}\cos(\phi\ +\beta)$$
$$where,$$
$$\phi = \frac{2\pi V}{VPF}$$
$$VPF = \frac{\lambda}{2\tau}$$

Where P is an optical power level, β is the phase angle between the signals, ϕ is the phase angle and proportional to the velocity of the surface [6-9]. The VPF is the known velocity per fringe constant and is measured in m/s/fringe. To solve for the velocity analytically the "a" and "b" parts of the signal are subtracted and β is forced to be $\pi/2$.

$$S_1 = S_{1a} - S_{1b} = 4\sqrt{P_{1a}P_{1b}}\cos(\phi)$$
$$S_2 = S_{2a} - S_{2b} = 4\sqrt{P_{2a}P_{2b}}\sin(\phi)$$

To solve for ϕ which will give the velocity, V, S_1 and S_2 must be divided.

$$\frac{S_2}{S_1} = \frac{\sin\left(\frac{2\pi V}{VPF}\right)}{\cos\left(\frac{2\pi V}{VPF}\right)} = \tan\left(\frac{2\pi V}{VPF}\right)$$

So,

$$V = \frac{VPF}{2\pi}\tan^{-1}\left(\frac{S_2}{S_1}\right)$$

In the event the phase angle β is not 90 degrees and the analytical method cannot be used, a single best fit solution to the two nonlinear expressions can be used at each time step to find the velocity. The VISAR diagnostic does not have the ease of use associated with PDV since it's based principally on free space optics. VISAR also incorporates large-core, multi-mode fiber. This fiber is used so that transmission optics can be easily changed between experiments and the light collection efficiency is improved due to the larger core fiber. In addition, the large core fiber scrambles the degree of polarization ensuring that the diagnostic is insensitive to variations in input polarization. However, this use of multi-mode fiber coupled with the use of a photomultipler tube (PMT) as a

detector gives VISAR about a 1 ns rise-time. The main advantage of VISAR is its ability to measure any velocity produced by land-based projectiles.

1.1.3 Single-Mode VISAR

The diagnostic described by this thesis was invented in response to a request to investigate the electronic components required to measure higher velocities using a PDV system, principally, the upgrade to higher bandwidth oscilloscopes. A PDV with 18 GHz system bandwidth could measure approximately 14 km/s velocities. However, the high bandwidth oscilloscopes required to reach this limit require significant electrical power and are very expensive ($120k each). At this point VISAR seemed to be the better option since it can measure any velocity produced by land-based projectiles. However, VISAR is a notoriously difficult diagnostic to implement. This resulted in an attempt to create a VISAR built out of PDV parts. PDV is advantageous due to its fast rise-time and ease of use but PDV lacks the ability to measure very high velocities. However, the main advantage of the VISAR diagnostic is the practically limitless maximum measurable velocity. This thesis describes a novel method of combining the positive attributes of PDV and VISAR into a more cost effective diagnostic called a Single-Mode VISAR (SMV). The new diagnostic will be a VISAR composed of single-mode fiber PDV components. The VISAR configuration will enable the measurement of any velocity produced by gas guns, high explosives, or any other method of producing a shock wave. The use of single-mode fiber rather than multi-mode fiber and free space optics enables ease of use and a fast rise-time.

This thesis describes the process of building and testing a single-mode VISAR. The tests were designed to confirm the performance of the diagnostic. These tests

include DC detector characterization which ensures that the photodetectors used in the SMV system will perform according to specifications. The SMV was also calibrated in order to confirm the performance of the system as a whole for three distinct types of velocimetry experiments. The results of each of these tests are documented. In addition, this thesis describes the operations required to prepare the SMV for an experiment. This process and examples of affirming results are included. Finally, the SMV was used to measure the velocity of a foil flier accelerated by a high voltage capacitive discharge in a spark gap. Chapter 5 contains the velocity data obtained, a summary of the results, and planned future work.

CHAPTER 2 SINGLE-MODE VISAR DESIGN

A single-mode VISAR diagram is shown in figure 2-1. The configuration is similar to VISAR and like the VISAR, SMV is a homodyned diagnostic. The concept is based on single-mode fiber optic components and fiber optic assembly techniques with low polarization dependence. This means that all components are un-polarized and have low birefringence. Such components are readily available in the near infrared wavelength regime.

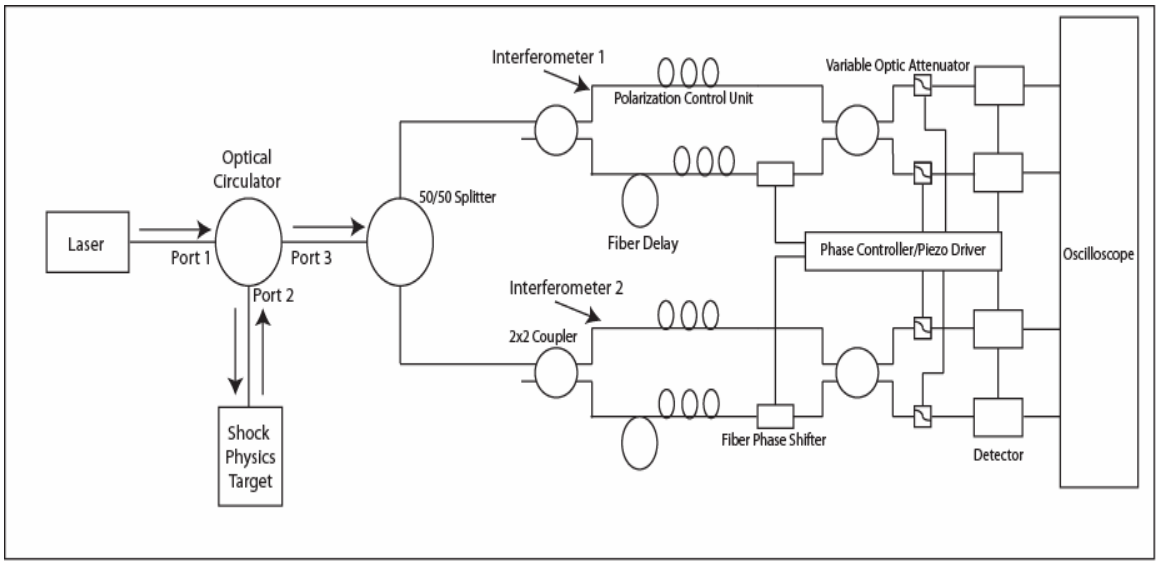

Figure 2-1 Schematic of the single-mode VISAR

Note that while the current design is based on near infrared components the concept is not restricted to a specific frequency.

A single frequency laser is required to produce light with a long coherence length. The light is coupled to a single mode optical fiber. The light is transmitted to an optical circulator via port 1 of the circulator. Laser light is transmitted over port 2 of the optical

circulator to the target material of interest. The moving target Doppler shifts the incident laser light and this Doppler shifted light is transmitted back through the optical circulator over port 2. The shifted and un-shifted light signals out of port 3 of the circulator are transmitted to a 50/50 optical splitter. This splitter divides the Doppler shifted laser light between two distinct Mach-Zehnder type interferometers. Each interferometer will split the light in half again and send each half of the light over a distinct path. The path difference corresponds to the velocity per fringe constant (VPF) of the interferometer. Selection of the fiber delay is used to establish the path length difference between the two legs in each interferometer. The length of this delay will depend upon the velocity range of interest and can be different in each interferometer. The length of each arm in the interferometer is governed by the lengths of the fiber components making up the interferometer. Using the components shown in figures 2-1, and 2-2 the difference between the two interferometer legs is 1.2m. The fiber delay can be changed by inserting a jumper consisting of a specified length of optical fiber into either leg of the interferometer.

Each interferometer has a polarization control unit in each leg to match the birefringence. The birefringence is adjusted to maximize the interference contrast and to remove polarization dependence of the signal amplitude. Since the velocity data is embedded in the amplitude of the interference signals the diagnostic must not alter this information in any way. Each interferometer also contains an all fiber phase shifter. The phase shifter is a commercially available, electronically controlled device that can continuously introduce several wavelengths of optical delay. Operating the phase shifter produces interference fringes at the detectors that are used to characterize the diagnostic.

Before a high speed velocity measurement is performed, the phase shifters are used to establish a fixed interference phase relationship between the two interferometers. The two signals from the paths of the interferometer are recombined at the second splitter where the two signals interfere. Each interferometer produces two interference signals. This interference produces modulation in the light amplitude and the modulated signals are detected and recorded by the detectors and oscilloscope.

In the present system, there are four optical outputs from the two interferometers. The four optical output power levels are detected and the electronic signals are recorded. The recorded data are analyzed using a non-linear simultaneous equation minimization process. One possible configuration of the instrument is to use two interferometer delays that are similar or identical and a relative interference-phase shift that is similar or identical to 90 degrees. Under these conditions, the 90 degree shift in the interference allows the data obtained from the diagnostic to be analyzed to obtain both positive and negative velocities, as would be produced in a vibrating target.

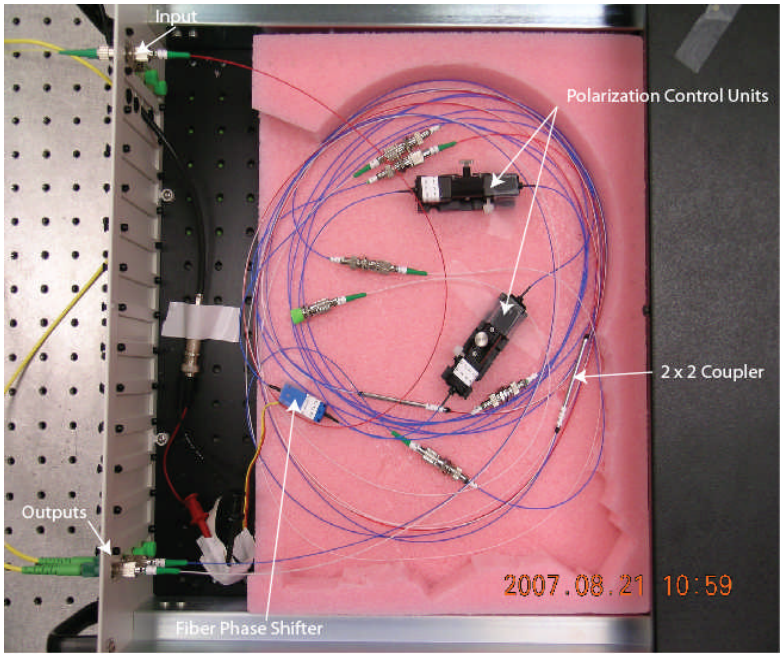

Figure 2-2 Single-mode VISAR intereferometer

Currently each interferometer is housed inside a rack mountable chassis on a pink foam block. The foam block is used to provide vibration and temperature isolation for the interferometer. As the first interferometer was constructed the need for vibration and temperature isolation became obvious when it was noted that the interferometer was sensitive to voices in the lab in addition to the air conditioning vent overhead. It is also important that there are no tight fiber loops within the interferometer. Tight fiber loops introduce a birefringence error that cannot be compensated for with the polarization control units. In addition, prior to any experiment or characterization the interferometer must be allowed to stabilize. The fiber jackets are stiff and will continue to relax after fibers are moved or jumpers added. This small movement will vary the birefringence and in order to match the birefringence between the two arms of the interferometer after any adjustment the diagnostic must be allowed a few hours to stabilize.

CHAPTER 3 SMV CHARACTERIZATION AND CALIBRATION

Before performing a velocimetry experiment with single mode VISAR certain operations must be carried out in order for the diagnostic to return quality data. These operations include both one-time measurements and measurements that must be conducted prior to every experiment. One-time measurements include detector characterization and interferometer calibration. DC Detector characterization verifies the linearity of the photodetectors. Interferometer calibration provides a measurement of the velocity per fringe constant and is necessary in order to verify the performance of the diagnostic in a particular velocity regime. During all of these operations the birefringence between the arms of each interferometer must be matched, this ensures that the diagnostic is insensitive to varying input polarization from the target.

3.1 DC Detector Characterization

The photodetectors used for the SMV diagnostic are New Focus 1592, DC to 3.5 GHz detectors. These detectors are specified to be highly linear over their frequency and power range. Since the data analysis makes the assumption that the electrical signals are linearly related to the light amplitude. For example, if the detectors saturate and the optical gain flattens at high powers [10], a sinusoidal curve can be compressed until it resembles a square wave. This effect would introduce an unwanted periodic source of error into the velocity measurement. Consequently, it is advantageous to have detectors that are linear over a specified power range so this type of error is avoided. Each detector was purchased with a frequency response curve, so we know that variations in the signal amplitude as a function of frequency will not be introduced. However, no vendor

information was provided on the linearity of the detector gain as a function of input optical power for either the DC monitor or RF outputs of the detectors. This characterization will verify that the detectors respond linearly to increasing optical power. Using an optical power monitor to observe the optical power incident from a CW laser operating at 1550nm onto the detector and a Tektronix 3032 oscilloscope to read the voltage output, both the RF and DC outputs were characterized over DC power levels ranging from zero to 700 microwatts.

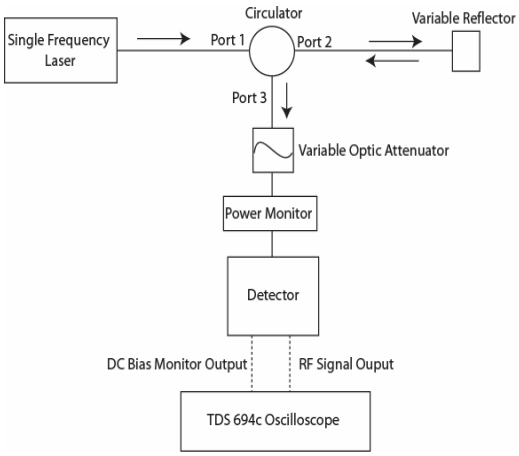

Figure 3-1 Detector DC characterization arrangement

3.1.1 Detector Characterization Data

The following plots depict the DC power response of both the DC, bias monitor output and the RF signal output vs the input optical power of each of the four detectors.

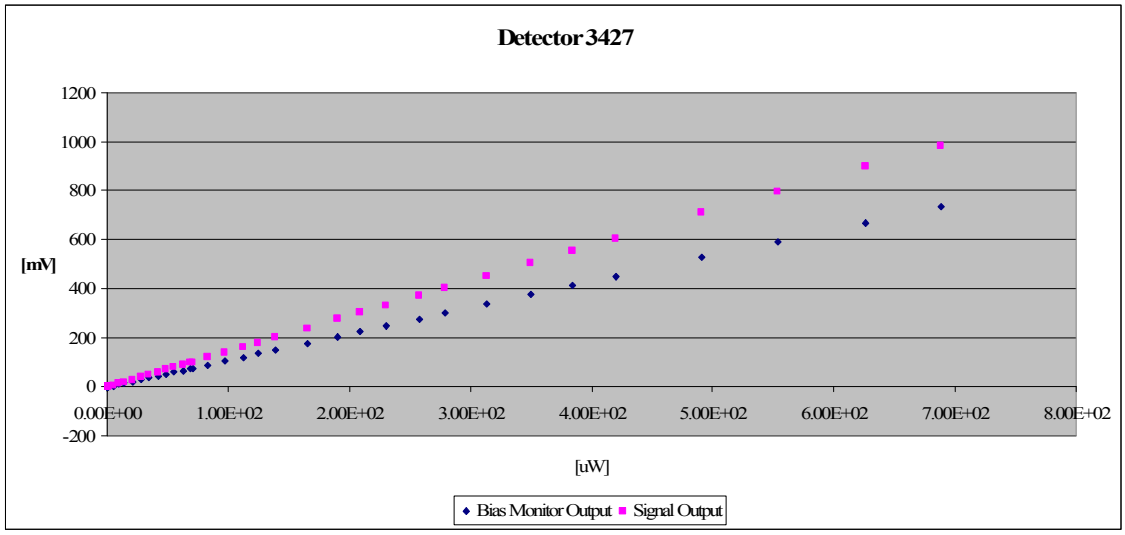

Figure 3-2 Raw DC characterization data for detector 3427

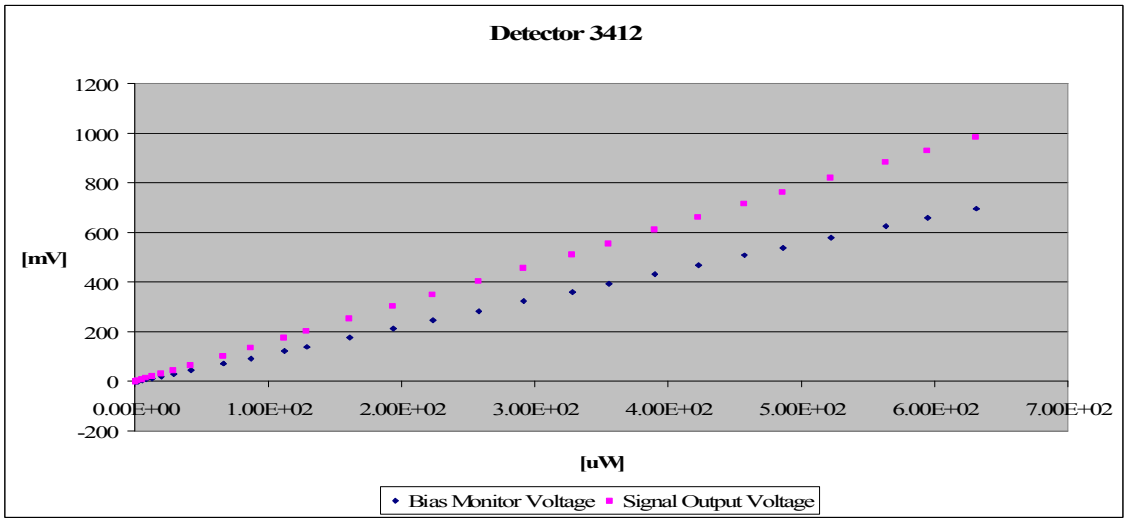

Figure 3-3 Raw DC characterization data for detector 3412

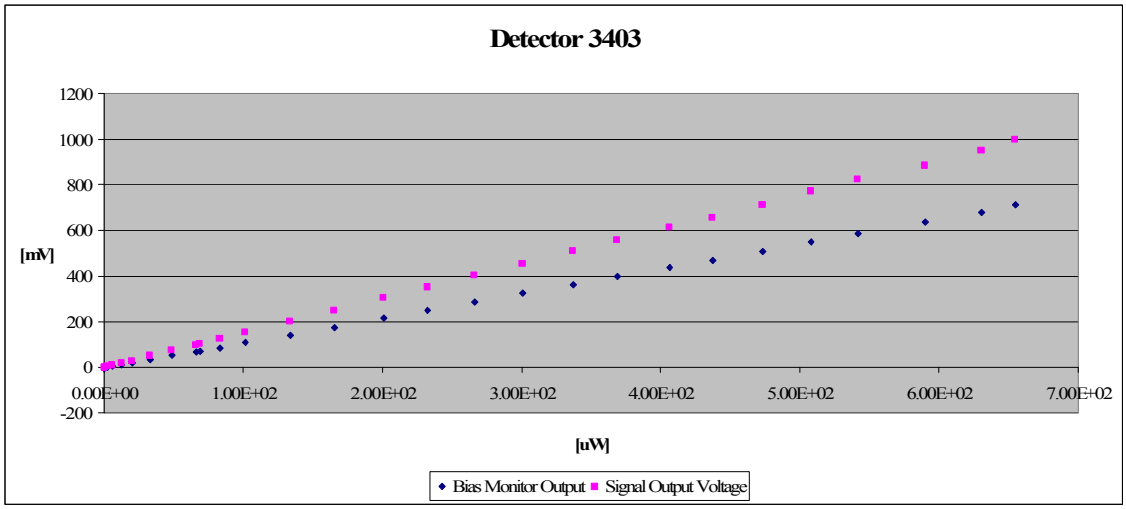

Figure 3-4 Raw DC characterization data for detector 3403

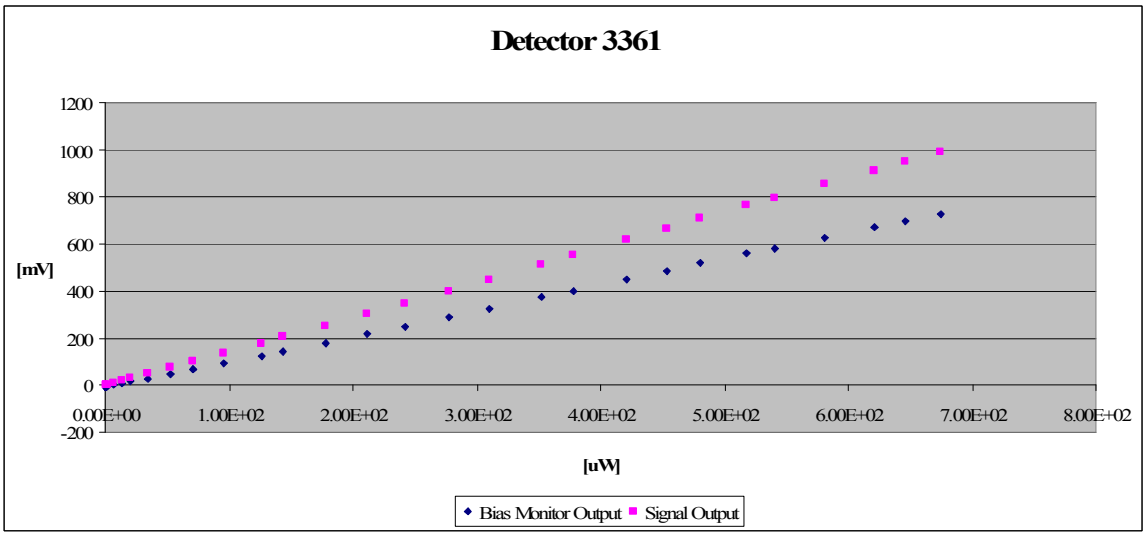

Figure 3-5 Raw DC characterization data for detector 3361

The detectors are all impressively linear and will not introduce any systematic errors individually. However, if the optical gain varies between detectors the data may still be impacted since during analysis the signals are combined. The next two plots are comparisons of the two outputs of each detector. Both the DC bias monitor and RF signal gains line up very closely. The fact that the gains are not only very linear but so

similar from detector to detector means that the data analysis will not be negatively impacted by errors introduced by the detectors.

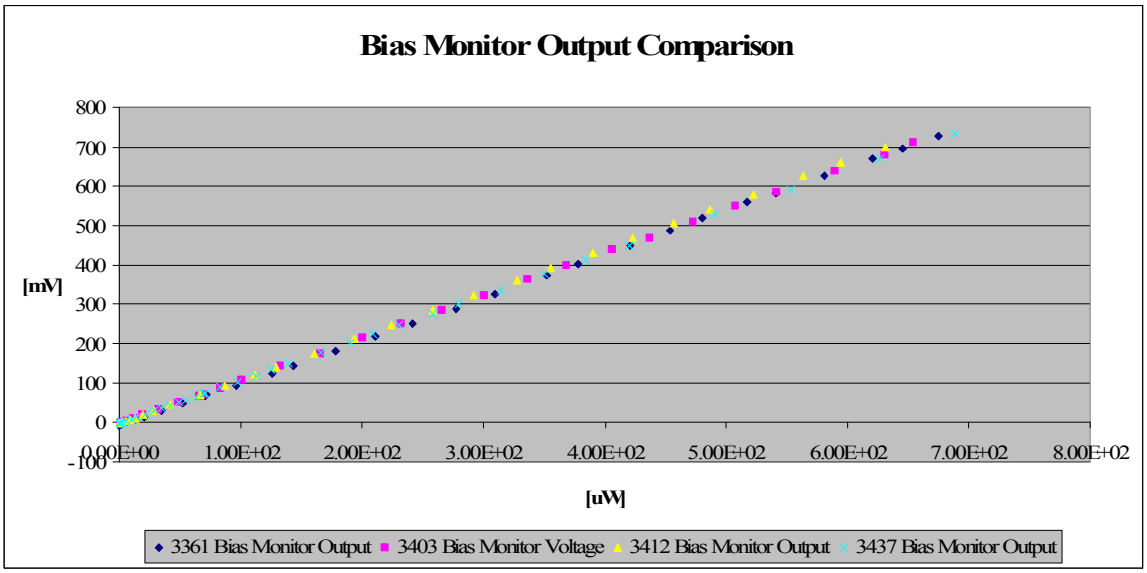

Figure 3-6 Comparison of the DC or bias monitor output of the New Focus photodetectors

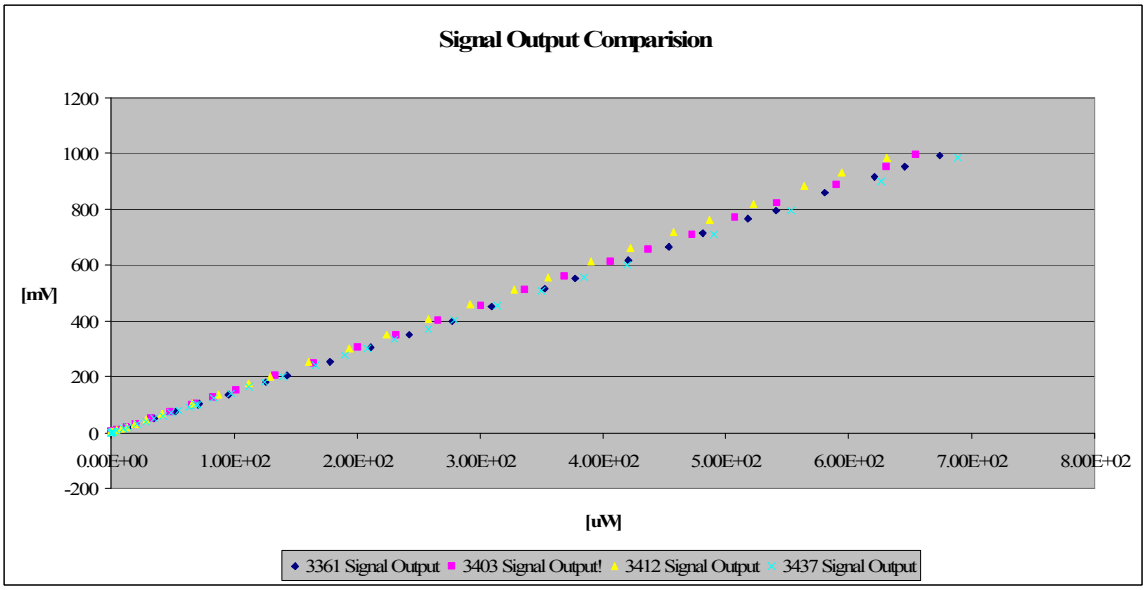

Figure 3-7 Comparison of the RF signal output of the New Focus photodetectors

3.2 Interferometer Calibration

3.2.1 Calibration Theory

Optical diagnostics measure shock or particle velocities by measuring the Doppler shift of the light signal as it is reflected back from the target. The expression relating the Doppler frequency shift and surface velocity is;

$$\frac{\Delta f}{f} = \frac{2V}{c}$$

Where, Δf is the frequency shift, f is the frequency, V is the velocity, and c is the speed of light in vacuum [11]. Since single mode VISAR is composed of interferometers, the frequency shift corresponding to one fringe due to the interferometer can be characterized by;

$$\frac{\Delta f}{c} = \frac{1}{(nd)}$$

Where, n is the index of refraction of the interferometer paths and d is the difference in length between the two legs of the interferometer. The expression for the time delay between the two interferometer legs is;

$$\tau = \frac{1}{\Delta f}$$

It should be noted that the time delay, τ, is the optical phase delay difference not the group delay [6]. The time and velocity resolution of the diagnostic is governed by these expressions and each experiment will have different requirements and the interferometer parameters must be varied to provide the desired data. These parameters are combined

into a velocity per fringe (VPF) setting which is specified prior to each experiment. The above expressions are combined to form the VPF expression.

$$VPF = \frac{\lambda/2}{\tau}$$

λ is the laser wavelength in vacuum [6]. A tradeoff between the time resolution and velocity error must be balanced for each experiment. The time resolution is similar to the time delay, τ , and the velocity error in the raw data is similar to the VPF divided by the signal to noise ratio. So a shorter VPF increases the time resolution but decreases the velocity error and longer VPFs provide increased velocity error but decreased time resolution. To set up the SMV for a specific VPF fiber jumpers are added to alter the path length difference in the interferometers.

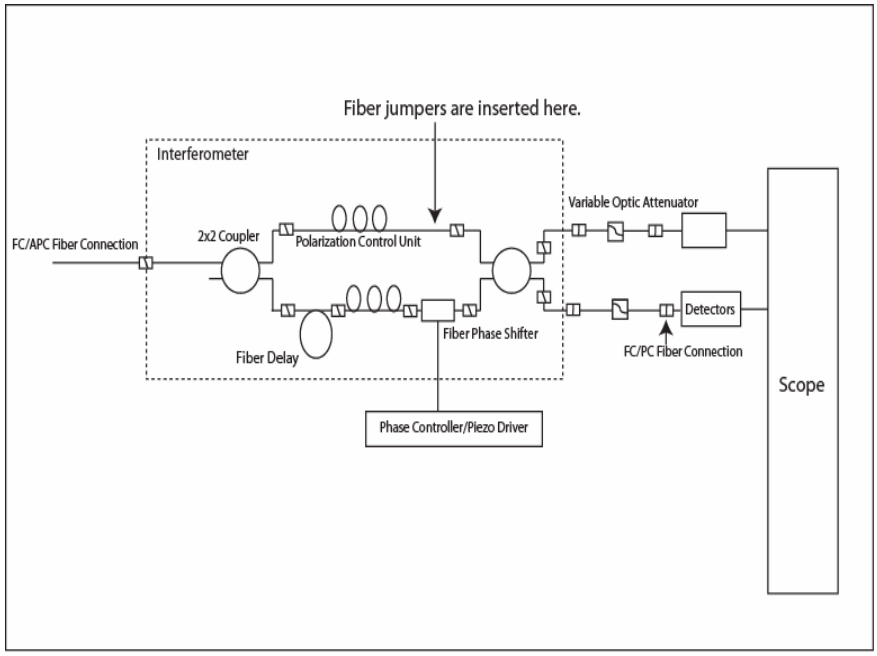

Figure 3-8 Location fiber jumpers are inserted to vary the VPF of the SMV

Since the time delay, τ , is the inverse of the frequency shift, Δf , measuring the frequency shift gives the velocity per fringe constant. Once these jumpers have been installed the frequency per fringe is measured to ensure that the VPF will provide the desired result. When a jumper is not inserted, the path length difference between the two interferometer legs is 1.2m or in terms of time delay, 6ns. Using this time delay, 6ns is the expected transient response time. This corresponds to a measured VPF constant of 122 m/s/fringe. In the current configuration the 3GHz oscilloscopes limit the bandwidth of the system. This corresponds to a response time of 0.13ns. So with an appropriately short time delay it is possible to obtain velocity resolution up to this 0.13ns limit in the present system. To complete the exploding bridge wire and gas gun velocimetry shots we selected 63cm and 1m fiber jumpers to calibrate in addition to the 1.2m path length difference.

3.2.2 Calibration Procedure

To confirm that the fiber jumper will provide a known VPF constant a calibration is required. This calibration is accomplished by sending tunable laser light to the interferometer and shifting the frequency of the tunable laser an amount corresponding to one full interference fringe.

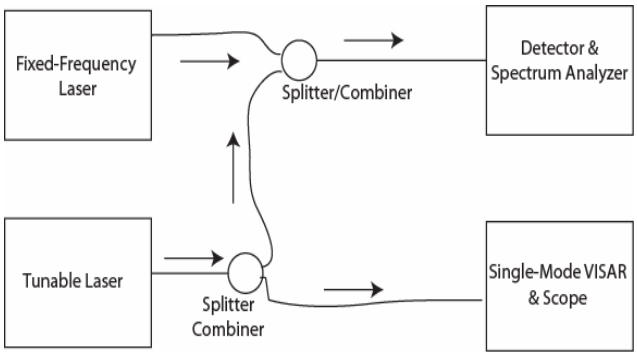

Figure 3-9 SMV calibration principle

This frequency shift is measured using heterodyned detection. The tunable laser light is split between an interferometer and a heterodyned detector where the shifted light is mixed with fixed frequency laser light. To perform the calibration, the set-up depicted in figure 3-9 is used. This calibration is performed individually on each interferometer after the fiber jumper has been inserted and the birefringence adjusted. The set-up incorporates two lasers operating near 1549.9nm, a fixed frequency and a tunable laser (the IPG laser and a New Focus 6328 tunable laser, respectively). The tunable laser signal is split and half the signal goes to the interferometer and the other half is beat with the fixed frequency laser to form a heterodyned beat signal. This beat signal is detected by the third high speed detector and displayed on the spectrum analyzer. As the tunable laser is tuned, the beat signal shifts on the spectrum analyzer. The other half of the tunable laser signal goes directly to the interferometer being calibrated.

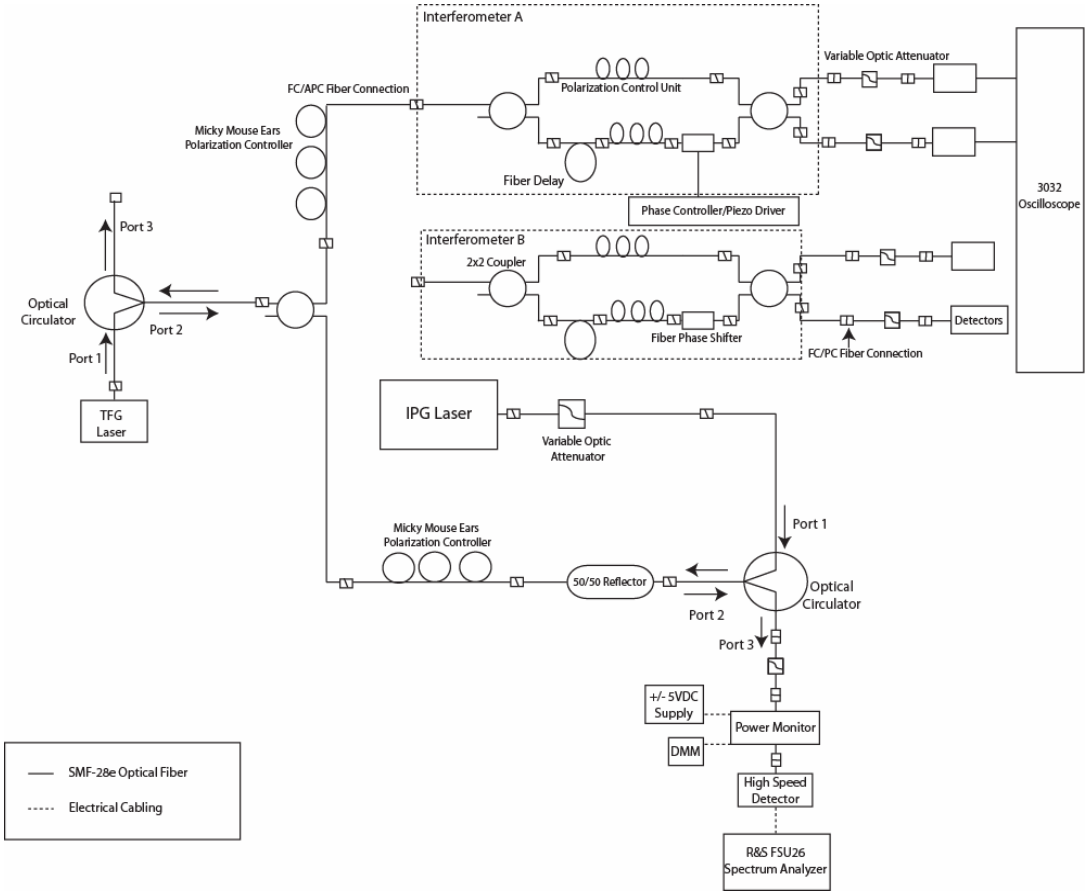

Figure 3-10 SMV calibration arrangement

The interferometers are both Mach-Zehnder type fiber interferometers. The two outputs of each interferometer are homodyne interference signals with phases 180 degrees apart which are detected by two photodetectors. The outputs of the two detectors are connected to an oscilloscope with an x-y display. Since the interference terms in the two arms of an interferometer are 180 degrees out of phase, the display shows a diagonal line if the phase shifter is on or if the laser wavelength is changing. Ideally, the display is a straight line with a negative slope.

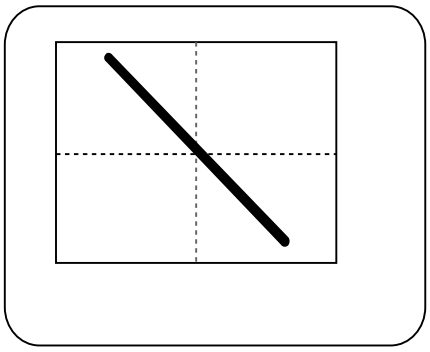

Figure 3-11 Sample of the oscilloscope display with phase shifter swept over several wavelengths of delay or with the laser wavelength varying.

If the phase shifter is held constant and the wavelength is stable, a slow diagonally drifting dot will appear on the display. This dot corresponds to the sinusoidal motion of the beat signal and moving the dot up, down and back up corresponds to moving over one full cycle of the sinusoid.

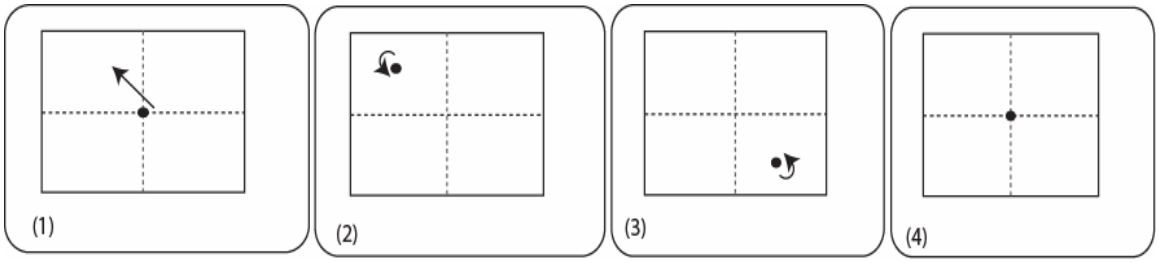

Figure 3-12 X-Y scope display through one upward cycle

To perform this calibration the dot is moved through one full cycle by adjusting the wavelength on a tunable laser and measuring the frequency shift of the heterodyne beat signal generated by the tunable laser as it is mixed with the fixed frequency laser on the spectrum analyzer. In figure 3-12 one full cycle is depicted; the dot begins in the center

of the display and moves upward, in (2) the dot peaks and comes back down, the dot moves through the trough in (3) and then returns to the center of the scope display. A high speed detector and spectrum analyzer measure the frequency shift in MHz. To perform the measurement the dot is set in the middle of the scope display and a "low" value is recorded off of the spectrum analyzer and then the dot is moved either up or down using the tunable laser and when the dot reaches the middle of the display again a "high" value is recorded. Typically, we begin with a low value and move to progressively higher values until we have adjusted the frequency through at least six to eight cycles of the interferometer. We calibrate in both directions to check for any systematic drift present in the interferometer. The data are then tabulated and the lows are subtracted from the highs to calculate the frequency differences or frequency shifts. These differences represent the change in frequency (typically in MHz) over one full fringe for that particular interferometer, jumper combination. The plots of the raw data are used to determine if there is significant drift over the cycle of the measurements as well as to compare different jumper-interferometer combinations. Table 3-1 shows the mean frequency shift for each jumper-interferometer combination as well as the standard deviation. Table 3-2 shows the measured velocity per fringe constants for each fiber jumper-interferometer combination.

3.2.3 Calibration Data & Results

The raw data sets are shown in the following plots. The plots are pyramid shaped with the high and low frequency measurements displayed for each interferometer-jumper combination. The data begin at low values and move up a fringe to a higher value. Once the peak is reached we begin at higher values and move down fringes to progressively

lower values. This gives the raw data plots the pyramid shape. The downward half of the pyramid has a more gently declining slope than the first, upward half. This is present to some degree in all the data and is likely due to inaccuracies in the piezo-electric motors in the tunable laser, fiber or phase shifter relaxation, or warming of the laser or interferometer throughout the calibration measurement. Because the measurement is made in two directions instead of one, the effects of systematic errors are reduced. The systematic errors tend to take the form of a slow drift and since this is the case, the error does not take place during the steps, it takes place between the steps. The period of time between the steps is much longer than the step interval itself.

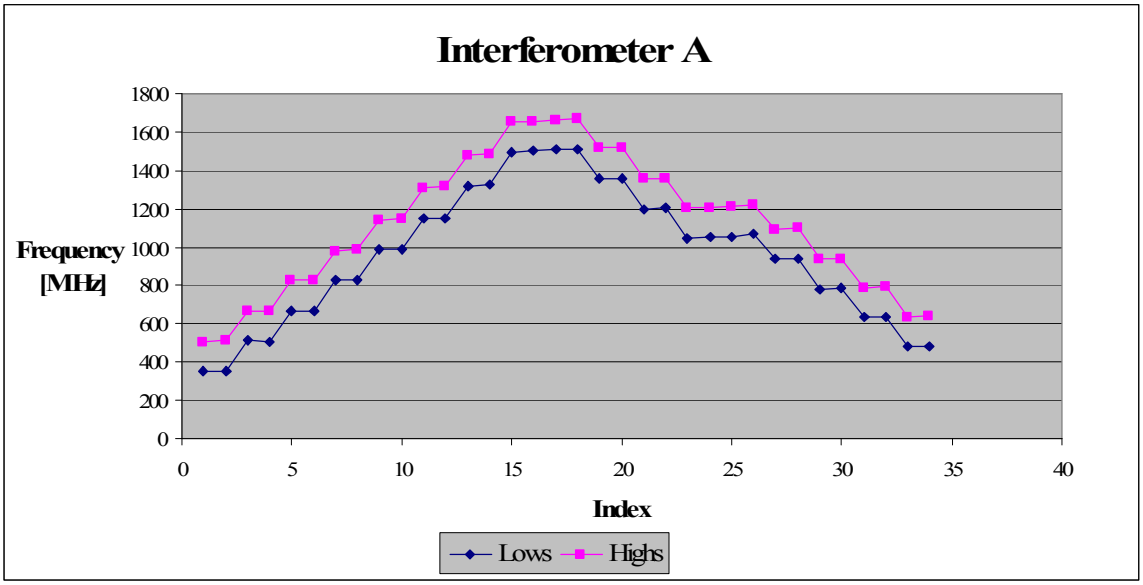

Figure 3-13 Interferometer A raw data without a fiber jumper inserted

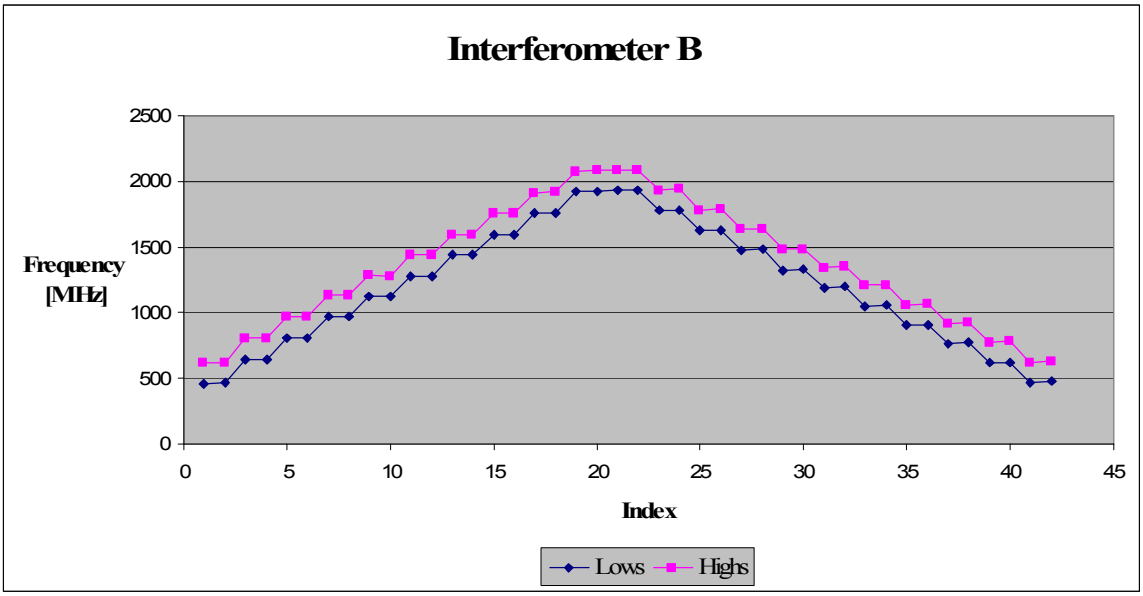

Figure 3-14 Interferometer B raw data without a fiber jumper inserted

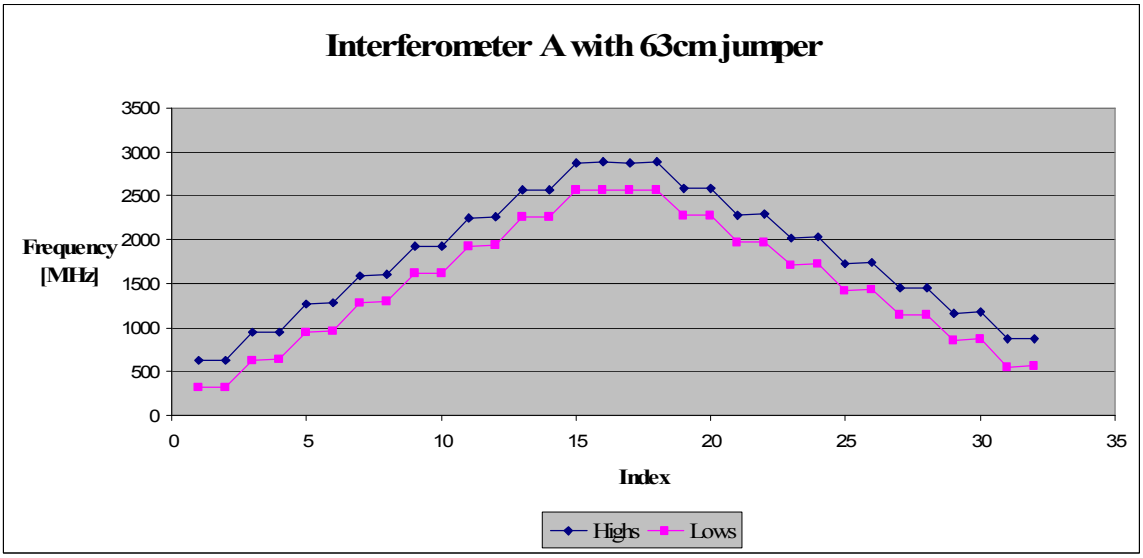

Figure 3-15 Interferometer A raw data with a 63cm jumper

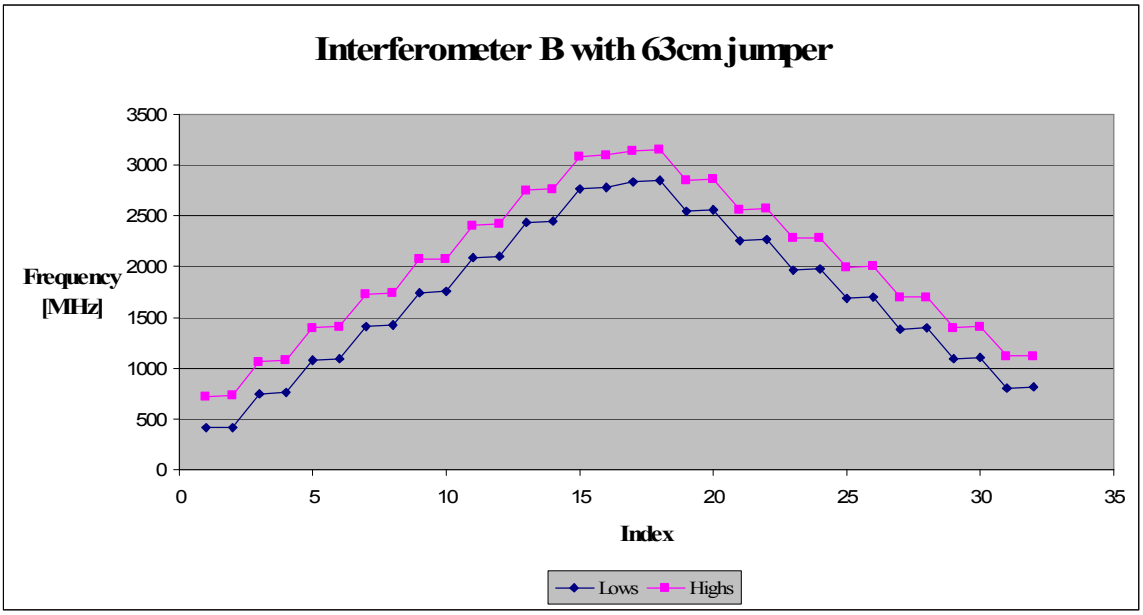

Figure 3-16 Interferometer B raw data with a 63cm jumper

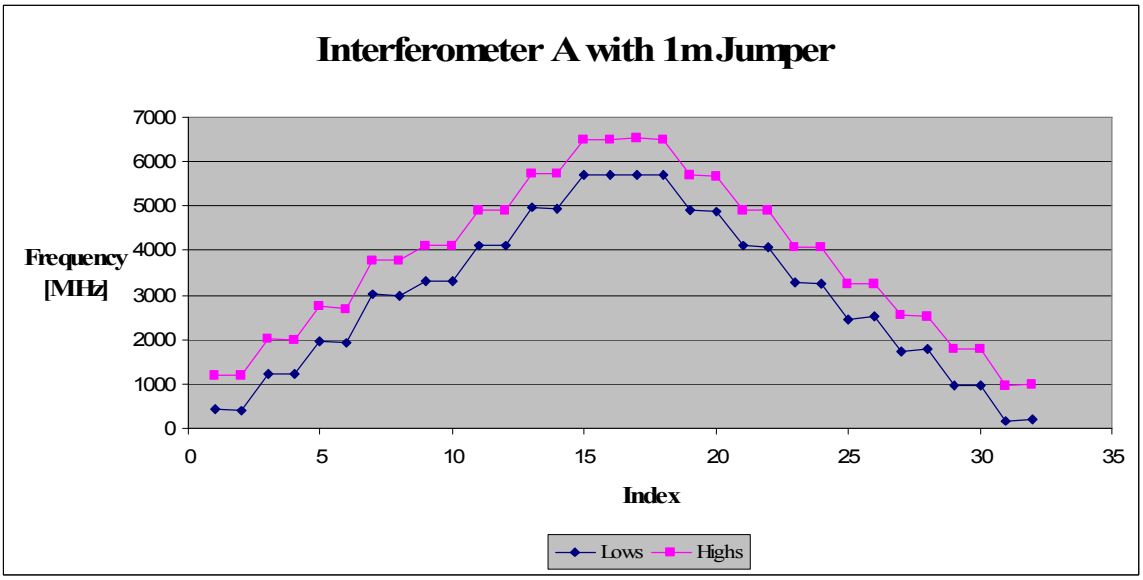

Figure 3-17 Interferometer A raw data with a 1m jumper

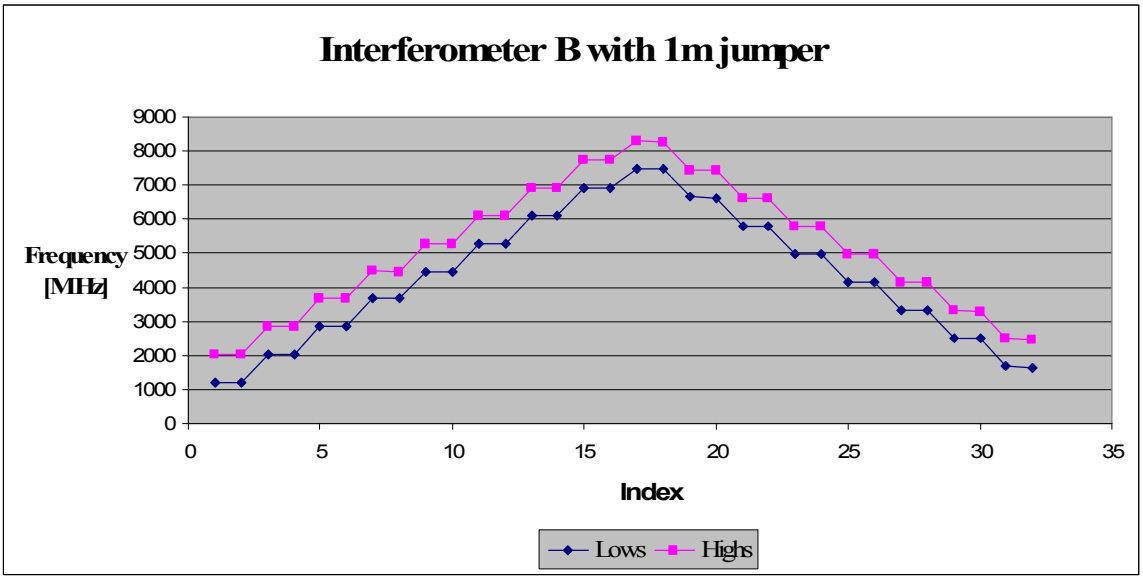

Figure 3-18 Interferometer B raw data with a 1m jumper

Figure 3-19 compares interferometers A and B without a fiber jumper inserted. Note that the mean frequency difference of the two interferometers differs by only 0.2 MHz.

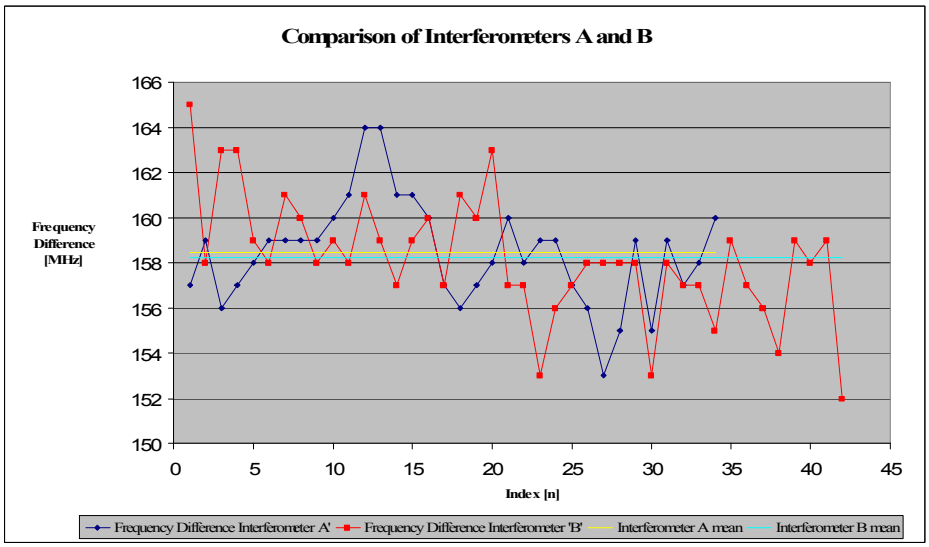

Figure 3-19 Comparison between the frequency shifts of interferometers A and B without a fiber jumper

The frequency difference corresponds to the shift in MHz to travel through one full fringe. The following plots (figures 3-20 to 3-22) show the measured frequency shift in MHz, with the mean and the mean +/- 1 standard deviation depicted.

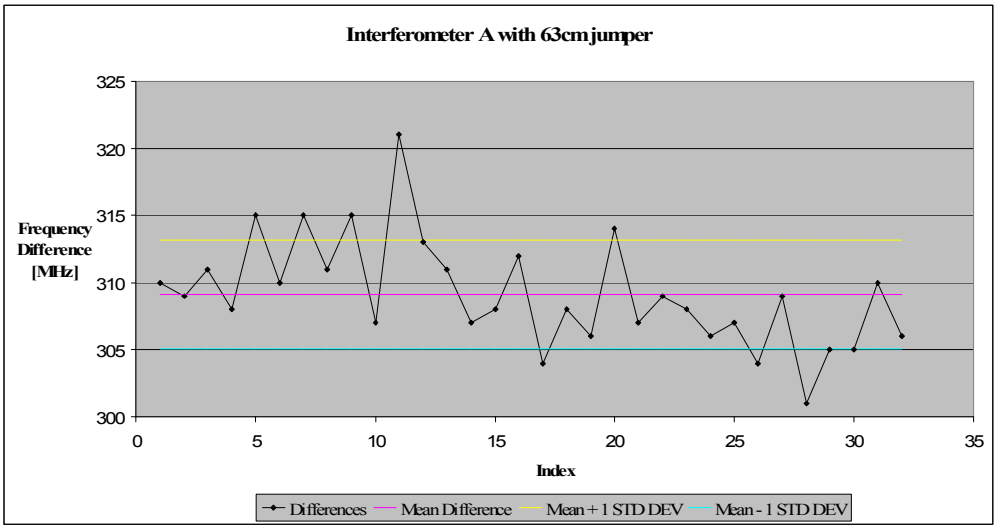

Figure 3-20 Measured frequency shift of interferometer A with a 63cm jumper

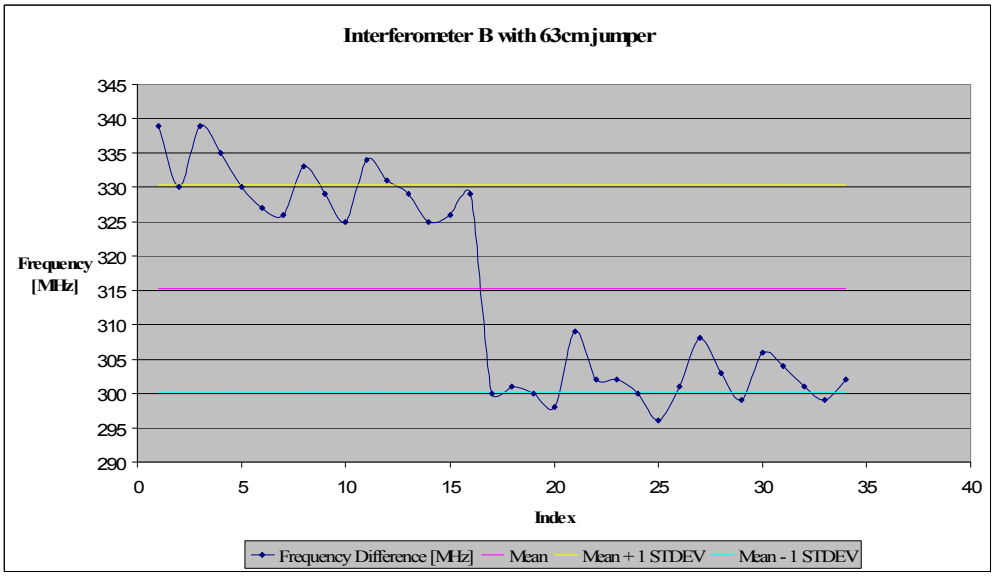

Figure 3-21 Measured frequency shift of interferometer B with a 63cm jumper

Figure 3-21 shows a profound difference between the frequency shifts going up and those shifts moving down. Figure 3-23 contains plots of the frequency difference in MHz along with the mean difference associated with each interferometer. Interferometer A with a 63cm jumper has a mean frequency difference of 309.1 MHz and interferometer B with the 63cm jumper has a 315.2 MHz difference. The difference between the A and B means is quite small, only 6.11 MHz, however interferometer B has a far more pronounced frequency difference when starting at a lower frequency and moving to a higher one than starting high and moving to a lower frequency. It seems that this phenomenon is present in each interferometer set-up but none are as profound as interferometer B with the 63cm jumpers. The poor results are believed to be the result of birefringence drift in the fiber during the measurement. Immediately prior to commencing the calibration we inserted the 63cm jumper. Fiber jumpers must relax for a few hours after being incorporated into the interferometer. This is necessary since the jacket on the fiber is quite stiff and will slowly relax. The birefringence cannot be properly matched if the fibers are moving and if the birefringence cannot be adjusted the calibration measurement will drift, so the interferometer must be allowed to settle.

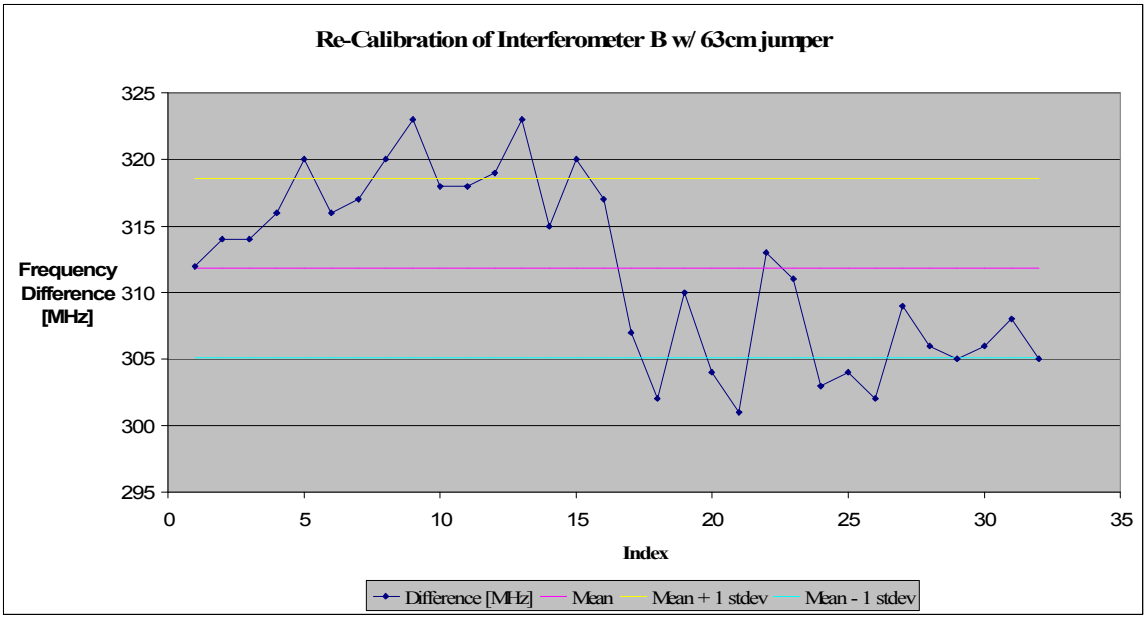

Figure 3-22 Re-measured frequency shifts of interferometer B with a 63cm fiber jumper

Figure 3-22 is the result of a re-calibration of interferometer B with the 63cm jumper after allowing the fibers to relax. This result agrees more closely with the other calibration results.

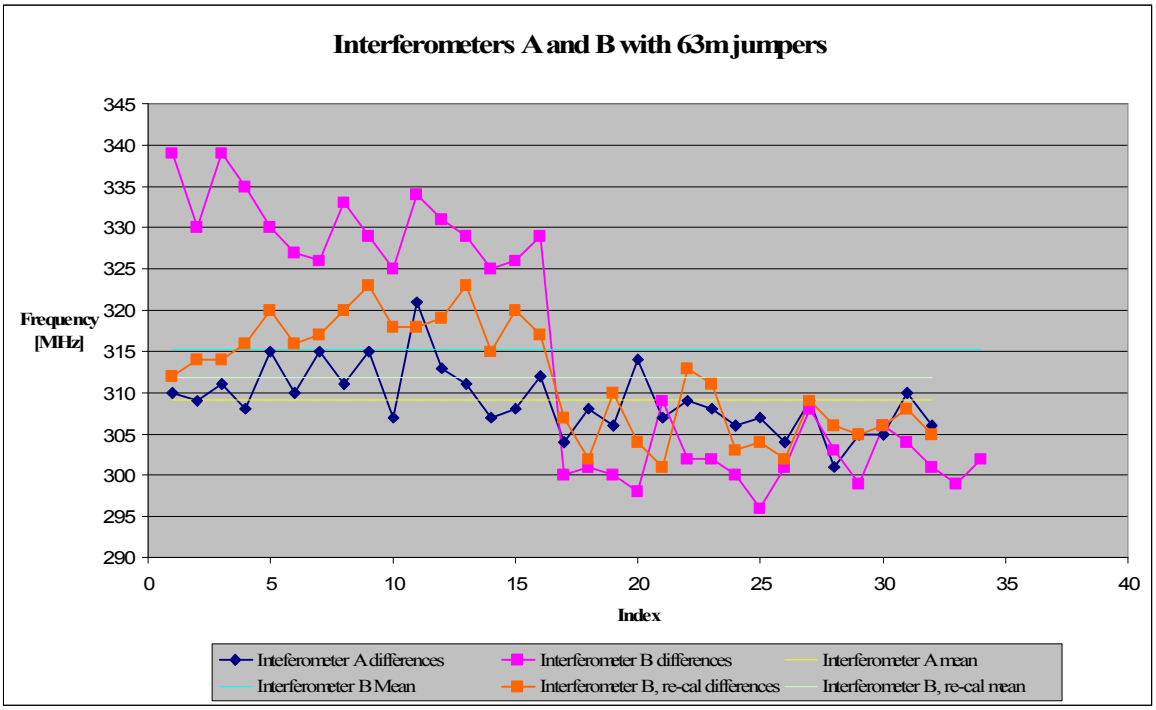

Figure 3-23 Comparison of interferometers A, B and the re-calibrated B with 63cm fiber jumpers

Although the step-like behavior is still visible it is far less pronounced in the re-calibrated data than the original data. We believe the step-like behavior present in the first calibration is due to interferometer drift. The original data were collected immediately after swapping jumpers. As a result, the jumper may have been relaxing during the measurement causing the drift. The jumper stabilized overnight prior to collecting the re-calibration data. Once the interferometers were calibrated with the 63cm jumpers, we calibrated the interferometers with 1m jumpers inserted.

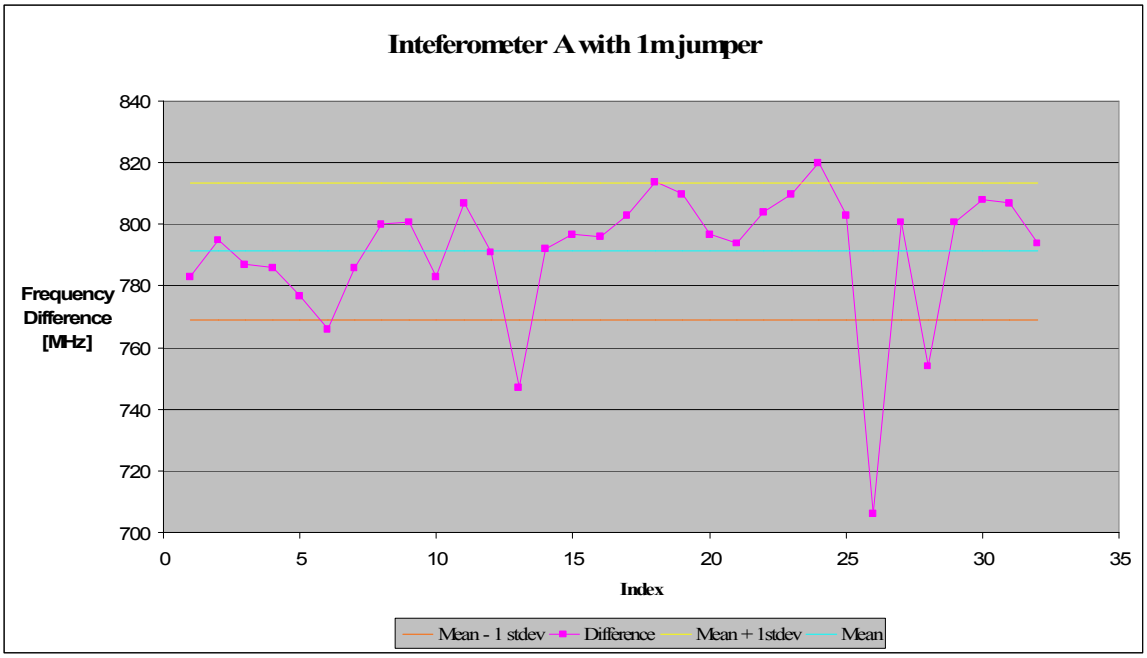

Figure 3-24 Interferometer A with 1m jumper

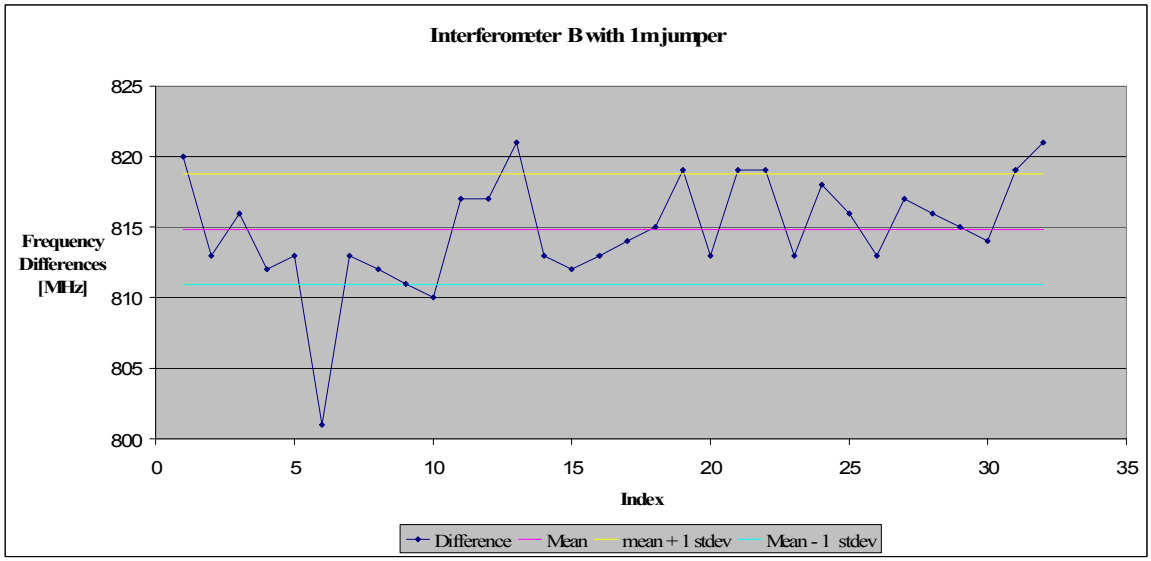

Figure 3-25 Interferometer B with 1m jumper

Table 3-1 Summary of interferometer calibration results

Interferometer/ Jumper	Mean Frequency Difference [MHZ]	Standard Deviation [MHz]
A	158.4	2.3 (+/- 1.45%)
B	158.2	2.6 (+/- 1.64%)
A / 63cm	309.1	4.05 (+/- 1.31%)
B / 63cm	315.2	15.0 (+/- 4.75%)
B / 63cm (re-calibration)	311.8	6.74 (+/- 2.16%)
A / 1m	791.2	22.3 (+/- 2.81%)
B / 1m	814.8	3.9 (+/- 0.47%)

Table 3-1 illustrates the mean difference of each interferometer/jumper combination and the standard deviation associated with each measurement. The percentages associated with the standard deviations represent the error contribution of the interferometer to the overall velocimetry measurement. These values are all below a few percent and each interferometer-jumper combination is considered ready for use in a velocimetry experiment. Table 3-2 lists the measured velocity per fringe constants for each interferometer/ jumper combination.

Table 3-2 Measured velocity per Fringe (VPF) constants

Interferometer / Jumper	Frequency Shift [Hz]	Tau [s]	VPF [m/s] (w/o window corrections)
A	1.58E+08	6.31E-09	122.76
B	1.58E+08	6.32E-09	122.61
A / 63cm	3.09E+08	3.24E-09	239.55
B / 63cm	3.15E+08	3.17E-09	244.28
B / 63cm (re-cal)	3.12E+08	3.21E-09	241.65
A / 1m	7.91E+08	1.26E-09	613.18
B / 1m	8.15E+08	1.23E-09	631.47

CHAPTER 4 SMV EXPERIMENTAL OPERATIONS

Once the detector characterization and interferometer calibration has been completed the diagnostic is ready to be prepared for the specific velocimetry experiment. This preparation must be performed prior to each experiment and consists of: choosing the VPF based on the desired velocity range and installing the calibrated fiber jumper into the interferometer chassis, matching the birefringence between the two arms of each interferometer, timing the diagnostic and aligning the fiber focuser to the target. Installing the fiber focuser into the target is of paramount importance since without proper alignment of the focuser the data signal will not be returned to the diagnostic. Timing measures the time difference between each interferometer output and provides a correction to the data analysis due to the time difference between fiber lengths. Matching the birefringence between the two arms of each interferometer will maximize the fringe contrast in the data and reduce polarization dependent error. These operations must take place a day prior to the experiment to allow the diagnostic to stabilize. If the fibers are moved inside the interferometer, the birefringence of the interferometer will drift until the diagnostic is stable. The quality of data returned will be detrimentally affected if the diagnostic is not stable at shot time, so the interferometers must not be disturbed within an hour of the experiment. Immediately before conducting a single-mode VISAR experiment the constant power levels must be measured for use during data analysis. Again, throughout all of these measurements the birefringence between the arms of each interferometer must be matched.

4.1 Matching the Birefringence of the Interferometers

During a velocimetry experiment it is possible for the polarization of the data signal to vary. Consequently, it is very important that the performance of the diagnostic is not detrimentally affected by these polarization variations. When the birefringence between the two arms each of the interferometer arms are matched the signal amplitudes of the single mode VISAR show little to no sensitivity to variations in input polarization. Matching the birefringence between the separate arms of each interferometer entails adjusting the polarization control units while monitoring the DC bias monitor output signal as the fiber phase shifter is shifting through several fringes and the input polarization is varied. The diagnostic must be in shot configuration.

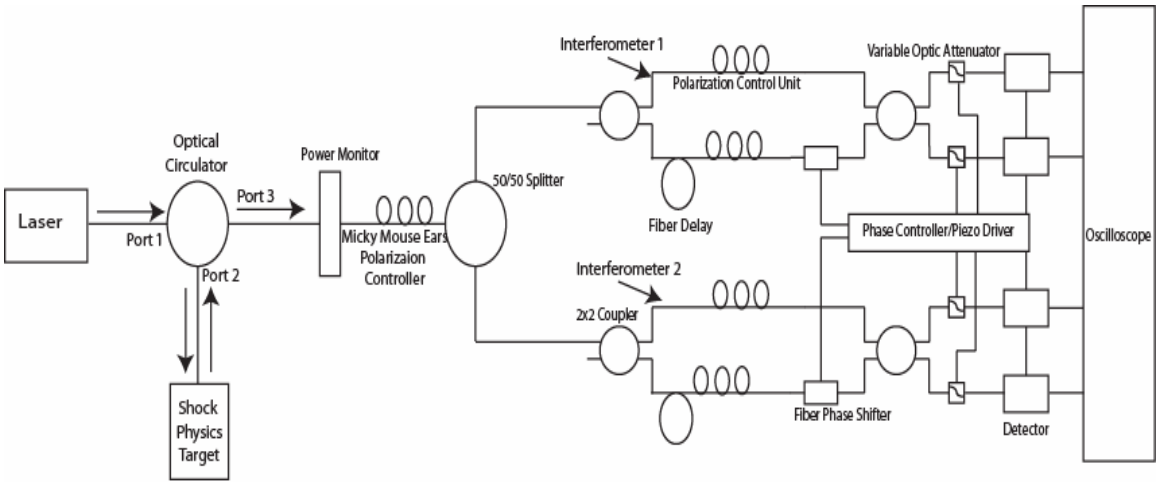

Figure 4-1 SMV experiment configuration

The two outputs of each interferometer are 180 degrees apart and are detected by the two photodetectors. The outputs of the two detectors are connected to an oscilloscope with an x-y display. Due to the 180 degree phase difference, the display shows a diagonal line if

the phase shifter is shifting through several wavelengths of delay. Ideally, the display is a straight line with a negative slope. When the birefringence is not matched between the two arms of the interferometer the ends of the negatively sloped line will increase and decrease as the input polarization is varied by adjusting the Mickey Mouse ears polarization controller. The birefringence between the two arms of the interferometer must be adjusted until the ends of the negatively sloped line no longer vary.

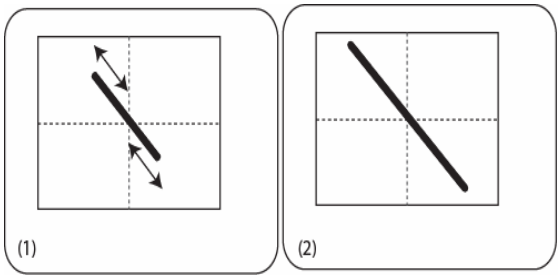

Figure 4-2 Sample of the oscilloscope displays showing (1) un-matched birefringence and (2) matched birefringence

Typically, we begin by adjusting the polarization controllers until the signal is canceled completely and only a small dot appears in the center of the scope trace. Next the signal is maximized using the polarization controller in one arm of the interferometer. At this point the birefringence is very close to being matched and only small adjustments are required on the polarization controller in the second arm. The birefringence between the two arms is matched once the ends of the trace no longer vary as the input polarization is varied. The birefringence will remain matched for a few days unless the fibers are moved within the chassis.

4.2 Timing

Timing characterization provides a correction factor to the experimental data which will compensate for differences in the fiber lengths outside of the interferometers. Consequently, this operation will decrease the overall error in the experimental results. SMV is timed in the shot configuration with two important changes to the system. The laser is moved to the target signal input position on port two of the circulator and the laser light is modulated. For this measurement a Mach-Zehnder style Lithium Niobate amplitude modulator was driven by a high speed pulse generator with the modulator interferometer phase adjusted by a DC bias. The overall rise time of this system was limited to 700 ps by the rise time of the electronic pulser. The longer leg of each interferometer is disconnected.

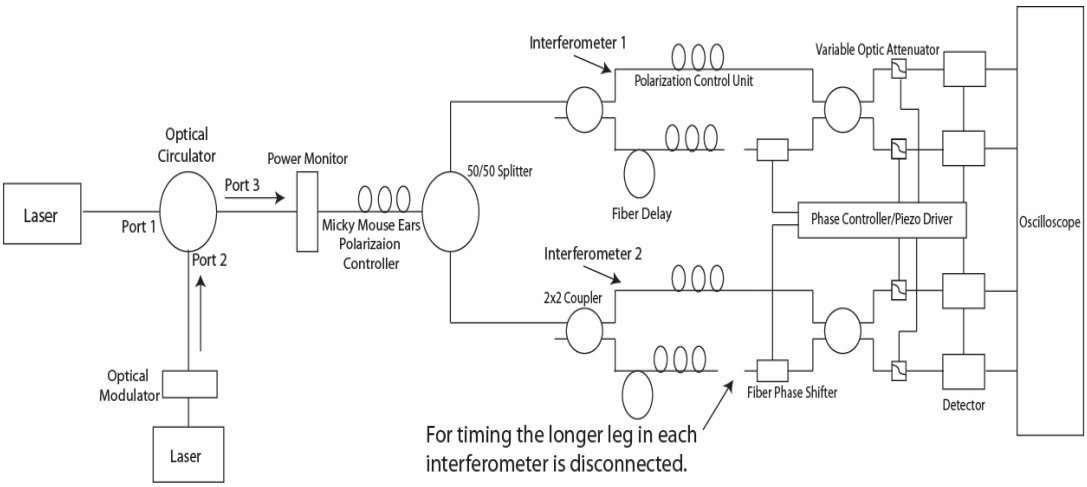

Figure 4-3 Equipment arrangement required for timing the SMV

This configuration will produce four pulses on the 3 GHz TDS 694c oscilloscope. In order to measure the time delay between each of the pulses the delay measurement on the

scope is used to measure the time difference between the earliest pulse and each of the three subsequent pulses. Typically these measurements are taken repeatedly and the results for each delay averaged. These differences are used to adjust the arrival time of the data signals and compensate for the differences in the fiber lengths. Note that the longest path length inside each interferometer is not included in this measurement; rather it is disconnected so that the pulses do not interfere. This measurement could be repeated with the shorter leg disconnected and the longer leg connected, however the difference between the two path lengths is accounted for during data analysis and actually measured during the interferometer calibration.

4.2.1 Timing Data

Table 4-1 illustrates typical timing data. In this case, scope channel three was the shortest channel. So we measured the difference between each of the other channels and channel three. Note that the actual length of any of the channels is not known, only their relative differences. In this particular instance channels three and four are significantly shorter than channels one and two. This difference is expected since the fiber lengths in channels one and two were approximately 7 meters longer than the jumpers used on channels one and two. Fiber jumpers with an FC/APC connector on one end and FC/PC connectors on the second end were required and four such jumpers of the same length were not available. This is an excellent example of why timing a system is a very useful exercise; any available equipment can be used and any time shifts present in the data introduced by mismatched equipment can be accounted for in the data analysis.

Table 4-1 Timing Data

Delay between	Ch. 3 and Ch. 1 [ns]	Ch. 3 and Ch. 2 [ns]	Ch. 3 and Ch. 4 [ns]
1	34.398	34.499	4.960
2	34.395	34.494	4.956
3	34.401	34.498	4.960
4	34.388	34.493	4.949
5	34.387	34.489	4.948
6	34.389	34.490	4.948
Averages [ns]	34.393	34.493	4.953

4.3 SMV Power Measurements

Immediately prior to beginning the experiment there are three measurements that must be made; a measurement of the zero offset power levels in the absence of the laser signal, the peak to peak power levels of each of the four signals, as well as the input power level while the peak to peak levels are measured. In addition, the power level of the return signal from the target as the experiment is executed is recorded using the power monitor. The power level as the shot commences must be recorded since the peak to peak levels may be measured at a slightly different power level than the power level at shot time and it is the recorded shot data which determines the initial phase during data analysis. All of these high-frequency parameters are used during the velocity data analysis. SMV data is analyzed in a method very similar to the way traditional VISAR is

analyzed. The interference equation which governs traditional VISAR also governs SMV.

$$I = I_a + I_b + 2\sqrt{I_a I_b}\cos(\phi_{ab})$$

Again the 'a' and 'b' signals oscillate at such a high frequency that they appear constant on the photodetectors and it is the phase that contains the velocity information. To compensate for the different gain and signal sizes, and loss differences between channels, a measure of the relative signal amplitudes is needed prior to each shot. These high frequency signals are measured prior to the shot so that the measurements can be used to isolate the phase of the interference term during data analysis. In order to measure the no-light levels the laser is fully attenuated and then for each data channel the snapshot and mean functions of the TDS694c oscilloscopes are used. To measure the peak to peak or 'B' light levels (where B = $2\sqrt{I_a I_b}$) the phase delay is swept through several fringes using the phase shifter's external control and a waveform generator is used to produce oscillations on the scope display. The oscilloscope's cursors are used to measure the peak to peak amplitude of each data signal. These numbers are recorded and saved for use during data analysis after the experiment. Figure 4-4 shows samples of the signals used to measure the zero-offset level and peak to peak power levels. Note that only one channel is depicted, four data channels are required for a single-mode VISAR velocity measurement.

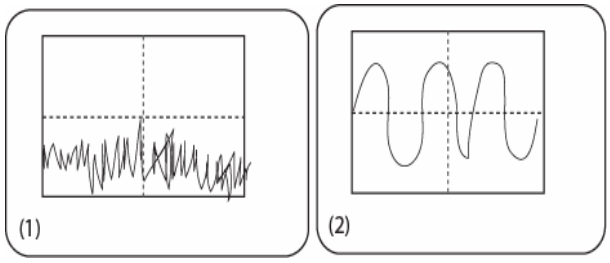

Figure 4-4 (1) Sample of the zero offset power levels, and (2) Peak to Peak, B power levels

Table 4-2 SMV Power Levels

Scope Channel	1	2	3	4
No Light Levels (mean in mV)	1.52	1.80	-1.52	0.52
Peak to Peak 'B' levels [mV]	102.0	101.6	98.0	101.6
Power level at shot, -3.37dBm				

4.4 Phase Measurements

As the experiment begins it is important that the phase difference between the two interferometers be set to approximately 90 degrees apart and held there. Since we know the peak to peak amplitudes, the power level at shot time, and the zero light offsets the data itself will provide a more exact measurement of the phase. However, it is important that the phase of each interferometer be set to opposite sides of a peak in order to ensure that the data can provide positive and negative velocity information, and that it can be analyzed unambiguously. For example, if the data from one interferometer is near a maximum or minimum (i.e. the phase sine or cosine is at 0) the uncertainty in the velocity will be infinite. If the phase of the second interferometer signal is about 90 degrees away (the sine or cosine is at 1) from the first signal, the signal from the second interferometer

can be used to extract the data. In order to set this phase difference, someone must use manual controls on the phase shifter piezo driver to maintain a 90 degree phase difference while monitoring the DC bias outputs of the photodetectors on a slow speed TDS 3032 oscilloscope. Currently, this phase difference is manually set. We attempt to hold the initial phase of one signal at -45 degrees and the initial phase of the second signal at +45 degrees for a total phase difference of 90 degrees. In practice, the phase difference can vary as much as +/- 10 degrees. However, since the recorded data provides a precise measurement of the initial phase, the variations do not have a negative impact on the overall velocity measurement. When the phase has been set and held, the experiment can commence. Setting the phase manually will only be done for the series of proof of principle experiments; eventually a feedback loop will be created to set the phase difference between interferometers. During testing, it was found that the piezo motors in the fiber phase shifters would experience excessive drift if the waveform generator used to drive the piezo controller was not off or if the piezo motors had been externally driven directly before attempting to set the phase manually. The piezo motors need ten to fifteen minutes to stabilize before attempting to set the phase difference between interferometers.

CHAPTER 5 EBW TEST RESULTS

5.1 Diagnostic Configuration

In order to demonstrate the operation of the single mode VISAR an exploding bridge wire (EBW) flier simulated a larger scale velocimetry experiment. An EBW uses high voltage capacitive discharge in a spark gap to create a very small ball of plasma which propels a foil flier at velocities around 200 m/s. To accomplish these shots the SMV was configured as shown in figure 5-1.

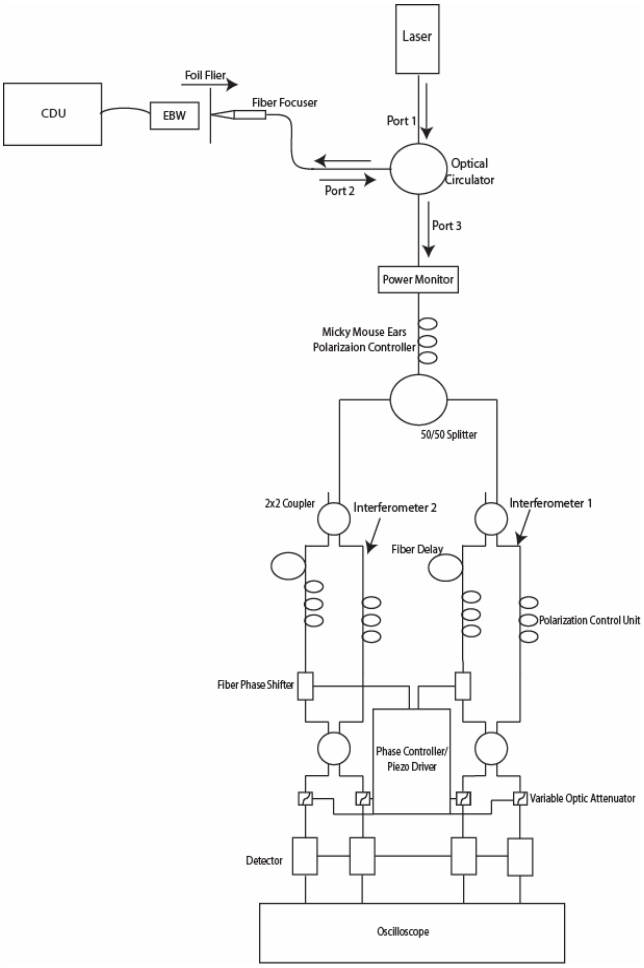

Figure 5-1 SMV configuration for the EBW shots

To accelerate the foil flier we borrowed a capacitive discharge unit (CDU) which would provide a one joule pulse to a Risi RP-1 exploding bridge wire. The bridge wire is shown in figures 5-2 and 5-3. The electrodes on the face of the EBW are originally connected by a thin silver wire. The same EBW can be re-used with a graphite pencil mark between the electrodes as a conductor. The foil flier was a strawberry nutri-grain bar wrapper cut to one quarter inch diameter circle. The wrapper was a 40 micron thick piece of aluminum or mylar sandwiched between layers of plastic. One side of the foil was more reflective than the other, so we chose to focus the laser signal onto this more reflective side of the foil.

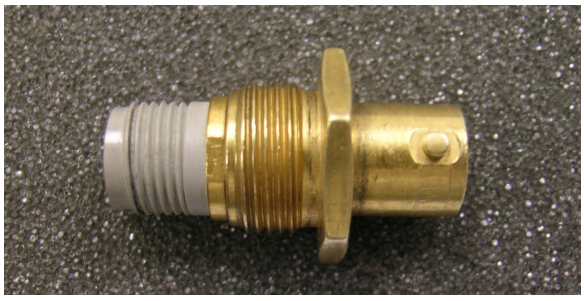

Figure 5-2 Side view of the Risi RP-1 EBW

Figure 5-3 Front view of the Risi RP-1 EBW showing the electrodes

The EBW and flier are loaded into a brass block and the focuser is positioned directly in front of the foil. The fiber focuser is placed in a tilt mount on an x-y-z stage so that it can be focused on the foil flier. A 1mm thick piece of lexan was placed between the fiber

focuser and the foil flier in order to protect the focuser from debris and allow for re-use of the focuser.

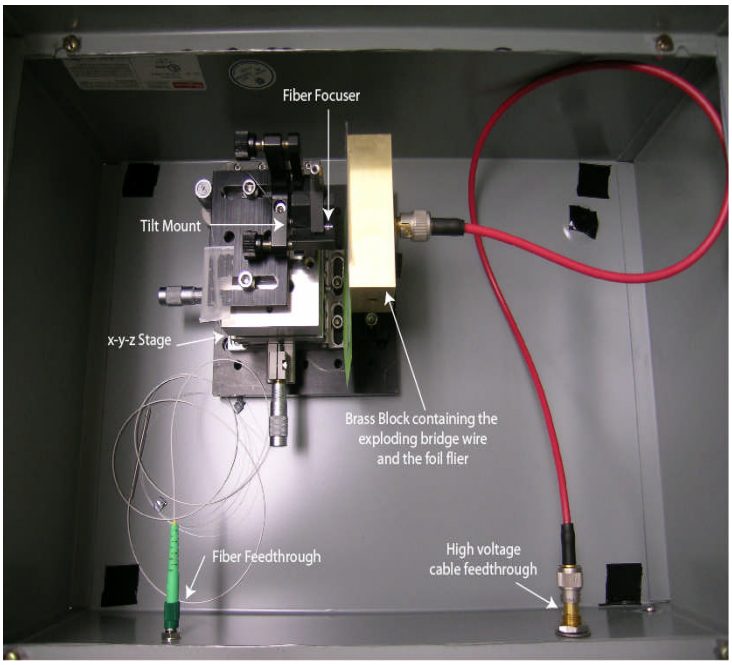

Figure 5-4 Shot configuration inside the EBW enclosure

It is important that this focuser have a very low back reflection (< -50dB) since the light shifted by the target must be at least 30dB greater than any other reflections in the system. For example, the circulator and target surface can produce an interference signal as the interferometer does. The signal produced by the target surface and circulator has a signal amplitude that is a few percent of the interference signal produced by the interferometer. This extraneous signal will not impact the overall velocity measurement as long as the return signal from the fiber focuser is greater than the 30dB specified. The probe used for the EBW experiments had a -51dB back reflection and a 16mm focal length. The flier was arranged so that the least reflective side was 1 to 2mm from the

spark gap and the more reflective side of the foil was 16mm from the focuser. To align the focuser to the foil flier a back reflection meter was used to maximize the return signal from the flier. In order to allow the probe to approach the optimum focus during the experiment the probe was pulled back from the foil flier until the back reflection decreased 1.5dB. Typically, EBW shots were performed with a -10dB or better return signal. The fiber focuser was connected to the single mode VISAR at port two of the circulator. The SMV diagnostic was used without a fiber jumper which gives a velocity per fringe constant of 122 m/s/fringe. This value was measured during the calibration of the interferometers. At this point, shot operations can commence. The zero-light, peak to peak, and shot power levels must be measured before the EBW can be fired.

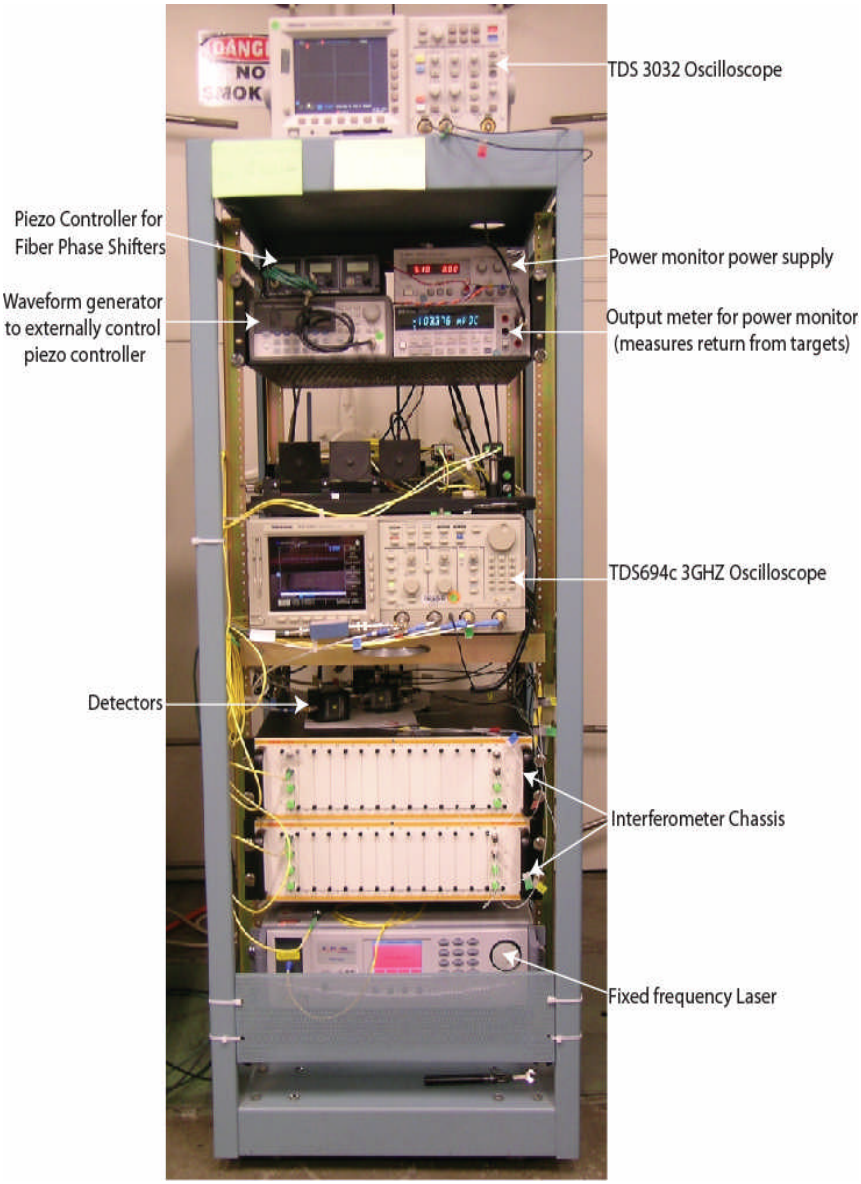

Figure 5-5 SMV equipment rack

5.2 EBW Data & Results

Prior to firing the EBW, the power levels required for data analysis were measured and as the EBW was fired, the phase was held to a constant value. An example of raw data is shown in figure 5-6. Channels 1 and 2 were the outputs of the first

interferometer and channels 3 and 4 were the second interferometer outputs. In this data set the 180 degree phase shift between black and red, and blue and green interferometer output traces is well illustrated at 1.5 microseconds. The 90 degree phase shift between the two interferometers is shown between the pairs of interferometer outputs. The blue-green set of traces lags the red-black set of traces by approximately 90 degrees. The noise that appears on each trace is due to high frequency phase noise in the laser. To determine that this was the case we observed the anti-correlation in the noise between pairs of signals, and by comparing the much lower noise levels with the interference absent. This noise is particularly apparent since the laser line-width seems to be several megahertz. Using a higher VPF would limit this noise since we would be operating at velocities much larger than the laser line-width.

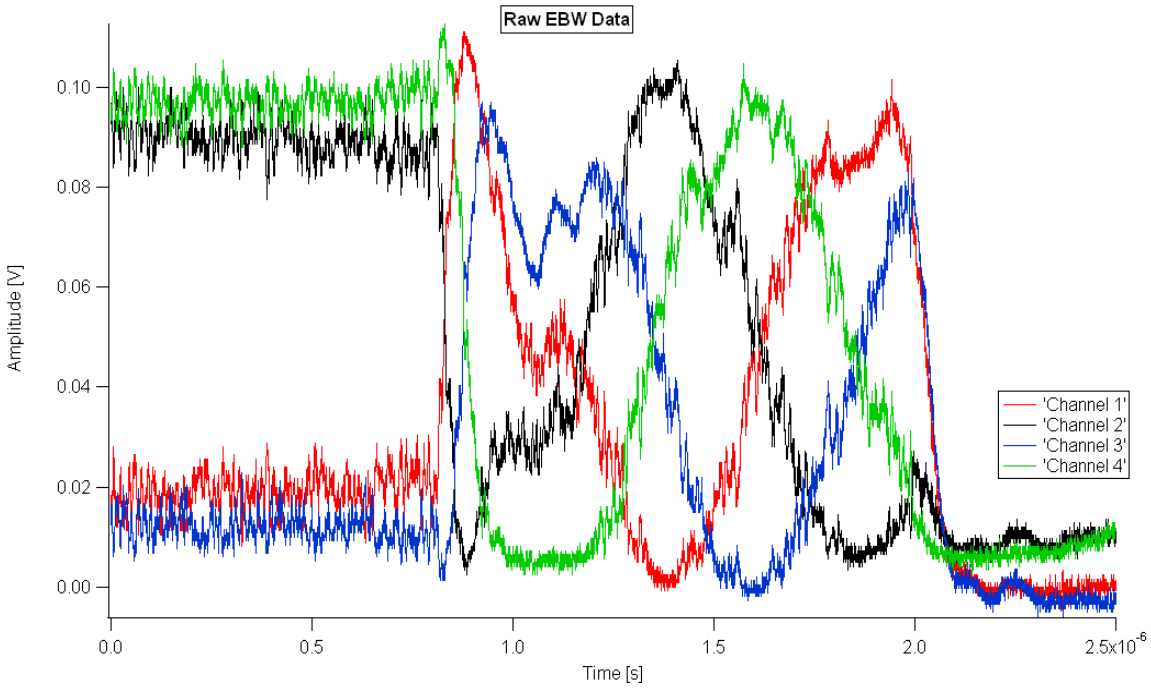

Figure 5-6 Raw SMV data from an EBW experiment

The data set shown in figure 5-6 was analyzed and produced the topmost trace in figure 5-7. This experiment was repeated several times and the results are depicted in figure 5-7. The velocity traces have been vertically offset for clarity. The bottom three traces show a fast velocity ramp to approximately 50m/s and then the signal goes out. This behavior is indicative of the foil bulging and then disintegrating. In contrast, the foil fliers in the top two traces did not disintegrate and a much longer velocity record was obtained. The second trace from the top actually had one of the four signals go off scale and the extra structure after the initial ramp is due to the signal loss not actual physics. The topmost trace that is not offset is the result of the data shown in figure 5-6. This data set is the best data obtained with the SMV to date. The foil did not fall apart and the signal did not go off scale. The trace begins like the others with a fast rise to 50m/s and then we see the signal flatten out for about half of a microsecond and then the trace accelerates to 200m/s. These tests demonstrate the ability of the SMV to measure velocities with a good degree of repeatability.

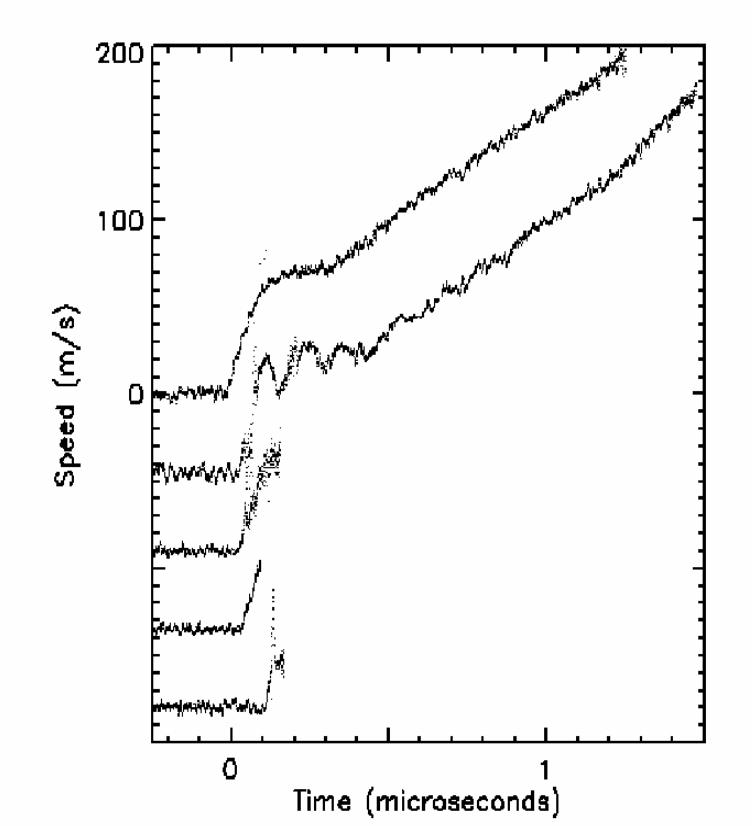

Figure 5-7 EBW velocity traces produced by SMV

5.3 Future Work

The work presented in this thesis represents the first iteration of the single-mode VISAR diagnostic. As this diagnostic was built, recommendations for future versions arose. These improvements include shortening the fiber lengths of the components inside the interferometers. This will make the diagnostic as a whole more compact and reduce birefringence effects. Along the same lines, future versions of this diagnostic will be fusion spliced where appropriate in order to eliminate unnecessary fiber connectors. Fewer fiber connections mean less fiber cleaning which makes the diagnostic easier to field on experiments. Later versions of this diagnostic may also employ components with tighter tolerances on the component specifications. Specifically the polarization

dependent loss on the 2x2 couplers should be reduced. Currently, the splitters used have a <0.15 dB polarization dependent loss. Theoretically, polarization dependent losses in the interferometer can add a significant systematic velocity error if the polarization from the target evolves. Matching the birefringence between the arms of each interferometer reduces the impact of any polarization evolution due to the target to less than a few percent. However, the <0.15dB polarization dependent loss can still introduce errors up to several percent if the polarization from the target significantly evolves. Note that such a significant evolution in the polarization in the data signal returned from the target represents a worst case scenario. In the future, studies should be conducted to examine the effects of residual polarization dependent loss on the velocity results. The results from this study will be used to set a limit on the polarization dependent loss permissible in the fiber components. Additionally, many of the SMV operations that are currently performed manually will be updated so that the operations are controlled electronically. In particular, the operation to set the phase between the channels at shot time should be updated with an electronic feedback loop so that the diagnostic does not require manual adjustments at shot time.

However, even without the improvements listed there have been invitations to participate in larger scale experiments. SMV will be incorporated into future velocimetry experiments in its current configuration since it performed well on the exploding bridge wire experiments. These experiments include a comparison of the SMV with a working PDV system on a gas-gun shot and a high explosive driven shot. These experiments provide an opportunity to compare the velocity data obtained by single-mode VISAR with data obtained by other velocimetry diagnostics in the km/s range. These

experiments will validate the method of calibration outlined in this thesis and the single-mode VISAR diagnostic as a whole.

REFERENCES

[1] Campbell, E.M., Holmes, N.C., Libby, S.B., Remington, B.A., Teller, E. (1997). The evolution of high-energy-density-physics: From nuclear testing to the superlasers. *Laser and Particle Beams, 15* (4), pp. 607-626

[2] Wasley, R.J, O'Brien, J.F., Henley, D.R. (1964). Design and construction of a new coaxial electrical pin. *The Review of Scientific Instruments*, 35 (4) pp. 465-46

[3] McMillan, C.F., Goosman, D.R., Parker, N.L., Steinmetz, L.L., Chau, H.H., Huen, T., Whipkey, R.K., Perry, S.J. (1987). Velocimetry of fast surfaces using Fabry-Perot interferometery. *Review of Scientific Instruments, 59* (1), pp. 1-20

[4] Lawrence Livermore National Laboratory, Sargis, P.D., Molau, N.E., Sweider, D., Lowry, M.E., Strand, O.T., (1999). Photonic Doppler Velocimetry. UCRL-ID-133075

[5] Strand, O.T., Goosman, D.R., Martinez, C., Whitworth, T.L., Kuhlow W.W. (2006). Compact system for high-speed velocimetry using heterodyned techniques. *Review of Scientific Instruments, 77,* 083108. Retrieved July 02, 2007 from http://scitation.aip.org/getpdf/servlet/GetPDFServlet?filetype=pdf&id=RSINAK000077000008083108000001&idtype=cvips&ident=freesearch&prog=search

[6] Hemsing, W.F., (1979). Velocity sensing interferometer (VISAR) modification. *Review of Scientific Instruments, 50* (1), pp. 73-78.

[7] Barker, L.M., Hollenbach, R.E. (1972). Laser interferometer for measuring high velocities of any reflecting surface. *Journal of Applied Physics, 43* (11), pp.4669-4675

[8] Barker, L.M. (1999). The development of the VISAR, and its use in shock compression science. In Furnish, M.D., Chhabildas, L.C., & Hixson, R.S. (Eds.), *Shock Compression of Condensed Matter* (pp. 11-17)

[9] Hecht, E. (2002). *Optics; Fourth Edition*. San Francisco, CA: Addison Wesley

[10] Palais, J.C. (2005). *Fiber Optic Communications* (5 ed). Upper Saddle River, NJ: Pearson Prentice Hall (pp. 226-229)

[11] Pedrotti, F.L., Pedrotti, L.S. (1993). *Introduction to Optics* (2 ed). Upper Saddle River, NJ: Prentice Hall

Appendix A SMV COMPONENTS

The tables below list the components used to build and test the SMV. These specific components are not required however components performing the same functions as those listed are necessary.

Table A-1 Components used to build SMV

	Component	Source
1	1550nm, CW, 2W, Fiber-Coupled Laser	IPG Photonics
2	1550nm fiber circulator	JDS Uniphase
3	Inline Fiber Power Monitor	EigenLight
4	2x2 Fiber splitter/ coupler	Thorlabs
5	All Fiber Polarization Control Units	General Photonics
6	All Fiber phase shifter	General Photonics
7	1592 DC to 3GHz Photodetectors	New Focus
8	PE34286 26.5 GHZ Electrical Cable	Pasternack
9	TDS694c 3GHz Oscilloscope	Tektronix
10	TDS3032B Oscilloscope	Tektronix
11	Variable optic attenuators	Oz Optics
12	Assorted SMF 28e fiber jumpers	Fiber Instrument Sales

Table A-2 Auxilary equipment required

	Component	Source
1	34401A Multimeter	Hewlet Packard
2	E3630A, Power Source 0-6 V, 2.5A / 0 +/- 20 V	Agilent
3	PCD-001, Piezo Controller	General Photonics
4	33250A 80 MHz Waveform Generator	Agilent
5	“Mickey Mouse Ears”-type Polarization Control Unit	Thorlabs

Table A-3 Equipment used during timing only

	Component	Source
1	AV1-V-HV1-C Electronic Pulser	Avtech
2	10020466 Modulator	JDS Uniphase